ChemElectroChem

Review
doi.org/10.1002/celc.202400377

Chemistry Europe
European Chemical Societies Publishing

www.chemelectrochem.org

Characterization of Porous Transport Layers Towards the Development of Efficient Proton Exchange Membrane Water Electrolysis

Genevieve Stelmacovich[a] and Svitlana Pylypenko*[b, c]

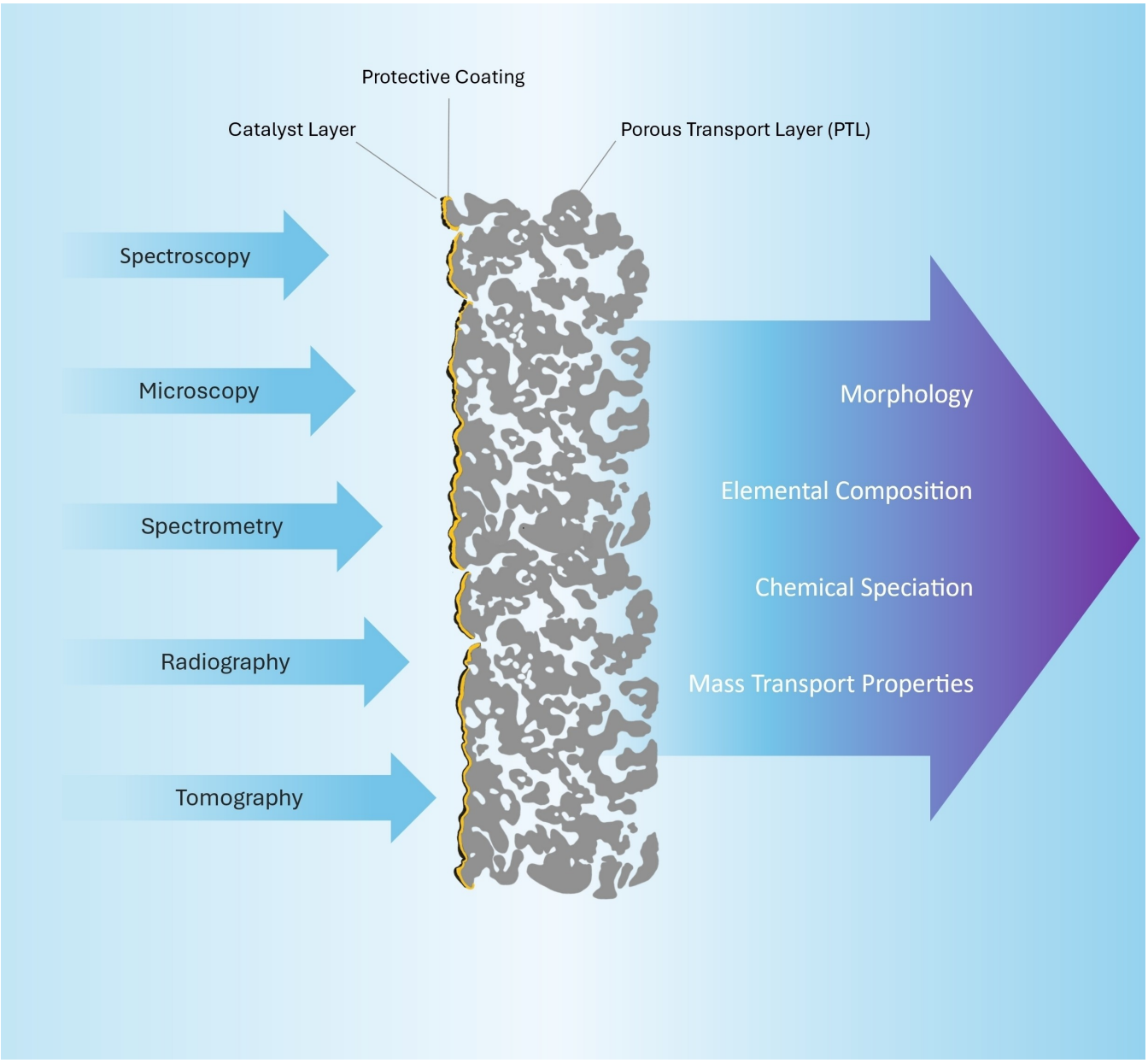

The current goals for implementing the hydrogen economy have highlighted a need to further optimize water-splitting technologies for clean hydrogen production. Proton exchange membrane water electrolysis (PEMWE) is a leading technology, but further optimizations of anode materials including the porous transport layer (PTL) and the adjacent catalyst layer (CL) are required to increase overall cell performance and reduce cost. This literature review describes advances in PTL development and characterization, highlighting early PTL characterization work and most common methods including capillary flow porometry and mercury intrusion porometry, optical imaging, neutron and x-ray radiography, and x-ray computed tomography. The article also discusses PTL protective coatings and their characterizations, focusing on platinum group metal (PGM)-based coatings, alternative non-PGM-based coatings, post-treated PTLs, and investigations into thin PGM-based coatings. Furthermore, it highlights the integration of the PTL and the adjacent CL along with associated characterization challenges. Lastly, this review discusses future developments in the characterization needed to improve PEMWE's performance and long-term durability are discussed.

1. Introduction

The world's energy needs are largely met through the use of environmentally harmful non-renewable energy sources such as fossil fuels. As universal energy demands and environmental consciousness increase, there is a world-wide push towards cleaner energy production, as demonstrated by many governmental and global programs and discussions.[1–4] The United States has joined the global initiative to introduce the hydrogen economy as a viable solution to this problem through government funded programs including the "hydrogen one-shot" and H2New consortium.[5] The integration of a hydrogen economy relies on three fundamental areas of infrastructure: hydrogen generation, hydrogen storage and delivery, and power generation. The hydrogen economy integrates clean hydrogen-based energy sources for transportation, industrial processes, and material production into the current energy infrastructure. This contributes to the overall energy infrastructure, mitigating the reliance on other energy sources.

Clean and renewable energy sources must replace current options, and this includes a reliable and efficient way to produce hydrogen. Currently, the most common approach for commercial hydrogen production is steam reforming, which is not sustainable or environmentally friendly and is commonly and colloquially referred to as "grey hydrogen".[3,6,7] The United States could significantly, if not completely, reduce its reliance on fossil fuels and other harmful energy sources through the implementation of a hydrogen economy with "green hydrogen" - or environmentally clean hydrogen production- through electrical water splitting.[8,9] The implementation of water electrolysis is the most realistic sustainable and environmentally friendly option to produce high throughput, high purity hydrogen.[7–10] Unfortunately due to cost constraints, currently water electrolysis is only responsible for 4% of all global hydrogen production.[3,11]

Water electrolysis is the electrochemical process of separating water into molecular oxygen and hydrogen. There are three main technologies, all of which undergo electrochemical water splitting under different conditions.[12] Alkaline water electrolysis (AWE) is well established and operates at lower temperatures (30–80 °C), but currently runs at limited current densities, limiting efficiency.[13] Solid oxide water electrolysis (SOWE) is conducted under higher operating temperatures (500–850 °C), utilizes non-noble catalysts, and promises high efficiency, but large-scale cell design is still under investigation.[12] Polymer electrolyte membrane water electrolysis (PEMWE) includes proton exchange membrane water electrolysis and anion exchange membrane water electrolysis.[14] Within polymer electrolyte membrane water electrolysis, the acidic media-based proton exchange membrane water electrolyzer (also abbreviated PEMWE) is a promising solution for clean hydrogen production for many reasons. Most significantly, the electrochemical cell's compact design and durability under elevated temperatures and high pressures allow high efficiency and durability in comparison to its competitors.[15] Additionally, this technique has relatively low hydrogen crossover rates, which increases the safety of the cell to be used commercially.[16]

PEMWE's have the potential to aid the transition to a clean energy infrastructure, but improvements in both material and manufacturing costs as well as optimization of performance must be realized to allow this device to be competitive for commercial hydrogen generation, assisting in the transition to a hydrogen economy. Cost analysis shows that one of the main expenses of PEMWEs at high production volume is material costs.[5] Most prominently, to overcome overpotential and degradation issues, the PEMWE heavily relies on platinum group metals based (PGM) materials, which are both rare and costly. Additional material costs associated with the use of titanium in the porous transport layer (PTL) and bi-polar plate (BPP) make the PEMWE too expensive to be competitive with the current energy infrastructure. In addition to reducing material costs, capital cost reduction will likely rely on improved manufacturing methods.[17] Currently, manufacturing these devices is time-consuming and complex, making mass production costs

[a] G. Stelmacovich
Chemistry Department, Colorado School of Mines,1500 Illinois St, Golden, CO, USA
[b] S. Pylypenko
Chemistry Department, Colorado School of Mines, 1500 Illinois St, Golden, CO, USA
[c] S. Pylypenko
National Renewable Energy Laboratory, 15013 Denver West Parkway, Golden, CO, USA
E-mail: spylypen@mines.edu

unreasonable in comparison to grey hydrogen production. Furthermore, the degradation of the electrochemical system- which impacts the lifetime and operation parameters of the system- is still under investigation. Several literature reviews on PEMWEs highlight the performance and durability of the overall system and present a comprehensive summary of PEMWE research development.[12,14,18–20]

It is important to note that the PEM fuel cell and water electrolyzer systems have many similarities but research efforts in water electrolysis are quite limited in comparison to PEM fuel cells. The knowledge resulting from research and development of the PEMFCs have a substantial impact on PEMWEs and are particularly helpful for the development of the cathode CL and gas diffusion layer (GDE), where the systems are similar. As optimization and improvements in the anode performance continue, cathode optimization also becomes a more significant area of research.

PEMWE drives water to be converted into oxygen at the anode through the oxygen evolution reaction (OER) and hydrogen at the cathode through the hydrogen evolution reaction (HER). This overall process is an endothermic reaction, highlighted by the following Equations (1–3) (Figure 1) where water, heat, and electricity are inputs of the device.[12,21,22] Produced oxygen is released as waste, whereas hydrogen is collected and used as a fuel source in many clean energy sources including proton exchange membrane fuel cells (PEMFC). A schematic of a PEMWE cell is shown in Figure 1. The membrane electrode assembly (MEA) is a 3-layered central component of the PEMWE. The three layers that make up this structure include the cathodic CL, typically an Ir-based OER catalyst, the anodic CL, typically Pt for the HER, and the proton exchange membrane, which is usually a perfluorinated sulfonic acid (PFSA) based polymer such as Nafion. All three of these layers are thoroughly researched both individually and as a combined MEA as they heavily contribute to overall PEMWE cost, performance, and durability.[19,23,24]

Most current efforts focus on the anodic catalyst layer (CL) and the adjacent porous transport layer (PTL). The PEMWE anode exists in an acidic environment with ranging temperatures up to 80 C.[20] Additionally, there is a high concentration of water and oxygen present, as well as high overpotentials. The combination of these parameters leads to a harsh environment, and many materials utilized in PEMFCs cannot be used in PEMWEs. Carbon easily corrodes into CO_2 at ~0.3 V, and therefore cannot be employed as a stable anode material. (Figure 2c) This affects both the CL and the PTL material, which also cannot rely on carbon-based materials. In addition to challenges associated with relying on unsupported material, the anodic catalyst must have high kinetic activity and stability under the acidic conditions of the anode. Iridium oxide is the current state-of-the-art anode catalyst, due to its promising stability and relatively high activity. Ruthenium oxides have also been explored as an anode catalyst material, demonstrating good activity, but very limited stability. A comparison of Pourbaix diagrams for Ir and Ru in a water system is shown in Figure 2, highlighting the stability of the materials of interest. Dissolution studies also demonstrate that though Ru has higher activity, degradation is too difficult to ignore.[25] Investigations of mixed metal oxides focus on combining Ru and Ir species, offering possible increased overall activity.[26] In addition to

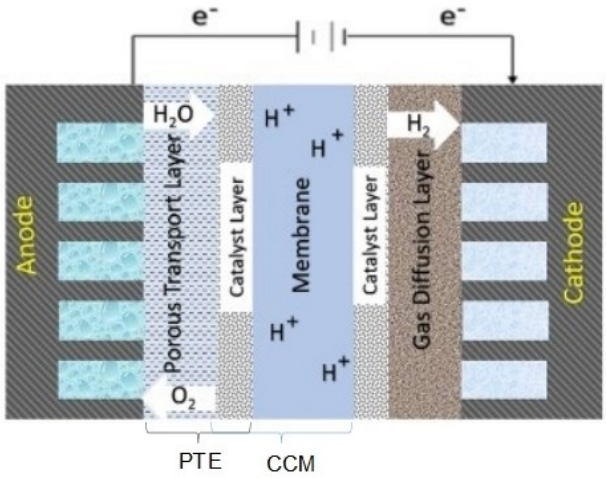

Cathode: $2H^+ + 2e^- \rightarrow H_2$ (1)

Anode: $H_2O \rightarrow 2H^+ + 1/2\ O_2 + 2e^-$ (2)

Overall: $H_2O \rightarrow H_2 + 1/2\ O_2$ (3)

Figure 1. Cross-sectional schematic of PEMWE.

Genevieve Stelmacovich is currently pursuing her PhD in the Chemistry Department at the Colorado School of Mines. Her research focuses on understanding the components of PEMWEs using various surface characterization techniques. She is also working on advancing the surface and interface characterization of PEMWEs by utilizing Time of Flight Secondary Ion Mass Spectrometry.

Svitlana Pylypenko is an Associate Professor in the Chemistry Department at Colorado School of Mines. She is also involved in the interdisciplinary Materials Science Program at Mines and holds a joint appointment at the National Renewable Energy Laboratory. Svitlana's research group focuses on investigating the surfaces and interfaces of applied materials. They emphasize building relationships between surface composition and structure, material properties, and performance. The group's research work involves multi-technique, multiscale analysis, and in-situ and operando studies bridging surface analysis, surface science, and catalysis.

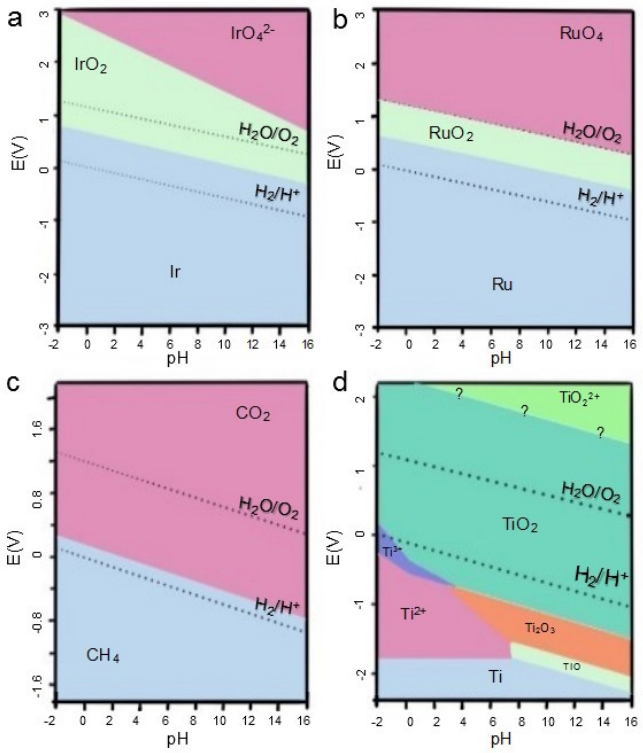

Figure 2. Schematic of Pourbaix Diagrams of a) Ir–O system b) Ru–O system c) C–O system, and d) Ti-Water system. Adapted from Ref. [30].

challenges with activity and stability, the catalyst must strive to be relatively cost-efficient, motivating investigation into catalyst loadings and fabrication methods. The complexities of the anodic catalyst and CL are discussed in several recent literature reviews, and therefore will not be highlighted in detail in this review.[26–29]

Since the anodic conditions of the PEMWE system cause the passivation of most materials, anode PTL's must be made of a material that has high corrosion resistance, high electrical conductivity, and enough strength to help support the electrolysis cell. The PTL connects the BPP to the CL mechanically, and as such the PTL material must be electrically conductive. Electrical conductivity plays a large role in the efficiency of the anodic materials in the PEMWE. Two major resistances in the PTL can lead to lower electrochemical performance in the cell. Firstly, the bulk resistance of the PTL, which can be affected by PTL material, structure, and thickness, inherently reduces the electrical conductivity of the PTL.[30] Additionally, the interfacial contact resistance (ICR) at the interface of the CL and PTL has been shown to directly affect cell performance.[31] Furthermore, hydrogen embrittlement can be an issue in these layers. Periodic trends of hydrogen embrittlement are Ti=Ta > Nb > Zr > graphite.[18] These combined factors resulted in the development of titanium PTLs, which are now the state-of-the-art PTL material, used commercially for most PMEWE anode PTLs.

Although titanium is the current state-of-the-art PTL material, there are still many concerns with its performance under operating conditions. Titanium naturally passivates to titanium oxide under the conditions of the cell. This is expected based on the Pourbaix diagram (Figure 2d).[32] This passivation can be visually identified as yellowish discoloration in tested Ti-based components.[33,34] The oxide layer significantly decreases the conductivity of the PTL, which decreases the efficiency of the entire PEMWE system. The added resistance of the oxide layer, specifically at the CL/PTL interface, leads to ohmic losses which contribute to the overall overpotential of the cell. To mitigate ohmic losses, PTLs are coated with a protective layer, which has been shown to significantly decrease ICR and maintain the structural stability of the cell.[35]

The cathode, typically composed of a carbon gas diffusion electrode (GDE) and a platinum catalyst, is of less concern.[5] Three main factors aid this statement. Firstly, the HER has faster kinetic activity than the OER, and as such is not a limiting factor of the system operation. Additionally, the complexity of mass transport through the porous matrix of the anode PTL slows down the OER reaction, adding more limitations to hydrogen ions reaching the cathode. Finally, the cathodic environment of the PEMWE has lower operating voltages and does not need the corrosion resistance that is required of the anode materials.

The traditional MEA fabrication involves the preparation of a catalyst coated membrane (CCM).[36–38] In this approach, catalyst is coated onto the membrane directly or through the preparation of a decal that is then transferred to the membrane. Deposition of the catalyst layer can be performed by hand painting or spray coating, and the community is developing more commercially viable manufacturing techniques such as screen printing. Much of the research in this area has been adapted from studies conducted on PEMFCs. Recent developments in fuel cell fabrication also involve roll-to-roll methods in which CL is deposited onto gas diffusion media.[39,40] Similarly, there are efforts to deposit CL directly to PTL to create the porous transport electrode (PTE).[41–44] A schematic of the PTE and CCM approach is shown in Figure 3.[24] Recent studies have shown that the PTE approach may be competitive with the

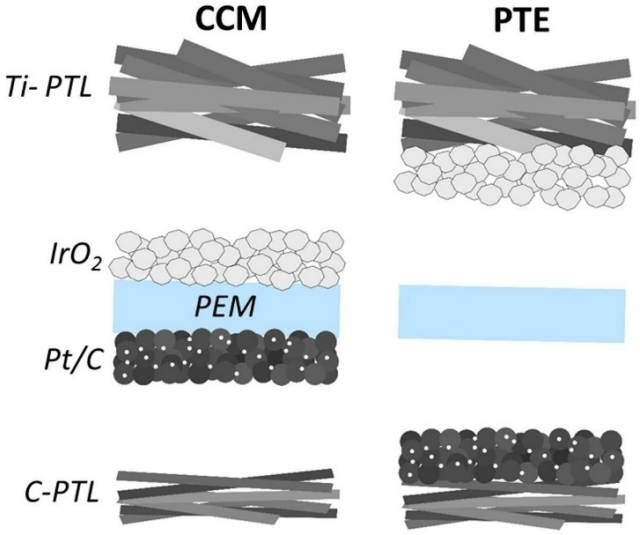

Figure 3. Schematic of CCM and PTE fabrication approaches. Reproduced with permission from Ref. [24].

historically used CCM approach, and as such currently both are investigated as viable options for large scale manufacturing.[45,46] A recent technical report by Nel Hydrogen shows that PTEs can better utilize low loading catalysts.[47] Further detail into recent anode engineering for the PEMWE can be found in Qiu et al.'s recent review.[48] Additional information about the specific fabrication methods utilized for low iridium loading MEA fabrication methods is covered in recent review by Wang et al.[49] Finally, recent efforts to improve the ICR at the interface of the CL and PTL have also targeted variations in MEA design.[24]

The main conclusions from the published literature indicate that the anode PTL and CL must be optimized to allow long-term, effective, and affordable commercial use of PEMWEs. As such, PEMWE research is heavily focused on performance and degradation analysis based on electrochemical testing. However, there is still a lack of detailed review highlighting the chemical and morphological properties and characterization of components, layers, and interfaces that exist in the PEMWE devices. Since the majority of the cost and performance issues come from the anodic parts of the cell, the characterization and optimization of the anodic components are particularly essential. The following sections of this review summarize non-electrochemical characterizations of the PEMWE anodic PTLs and PTLs integrated with CLs.

2. The Porous Transport Layers and Characterization of Their Properties

Initial PEMWE research efforts and publications, spearheaded by the General Electric company in the 1970's, were based on battery systems and included a current collector, which allowed the transport of molecules, atoms, and electrons to and from the channel to the anode catalyst layer of the cell.[50] The term current collector continued to be used until the mid-2010's, when the terminology was changed to the porous transport layer (PTL) to describe the layer more accurately. Throughout this review, PTL terminology will be used for consistency, regardless of the source terminology. Additionally, the literature commonly interchanges GDE and PTL when referring to the carbon gas-diffusion layer at the cathode. In this review, the cathode layer will be referred to as GDE. As such, any time the PTL is referenced, it will be referring solely to the anodic PTL.

One of the main functions of the PTL is to ensure good mass transport. Primarily, the PTL's purpose is to allow water to flow from the inflow channel to the where the OER occurs. From there, hydrogen ions are transported to the cathode, where the HER occurs. Oxygen, which is a byproduct of this reaction, is transported back through the PTL to the channel, where it is omitted as waste. Oxygen build-up throughout the PTL could lead to mass transport issues, as it slows the rate at which water can reach the CL. This results in a slower rate of hydrogen production, which ultimately decreases the overall efficiency of the PEM device. As such, morphology of the PTL, including parameters such as pore size, pore size distribution, porosity, and tortuosity all affect how efficiently oxygen can leave the system. It may seem that a plausible solution to improve mass transport is through increasing porosity to allow oxygen to leave the system more efficiently. However, larger pore size, or higher in plane porosity, and lower tortuosity were found to consequentially lower electrical conductivity, decreasing overall efficiency of the system. As such optimization of the morphological structure of the PTL is more complex, hence the need to pair morphological analysis with electrochemical performance analysis.

There are four known morphologies for PTL's: felt,[51] mesh,[52,53] foam[54,55] and sintered.[44] Typical commercially produced titanium PTL's come in two forms: a felt titanium sheet or sintered titanium. Note that due to inconsistency in publications within this field of research, the felt PTL is similar to the mesh PTL material that is typically produced in a lab setting; the same can be said about the foam and sintered PTLs. The morphology and structure of PTL's has been characterized by a variety of techniques. Each of the techniques provides valuable information and a combination of techniques is required for a truly comprehensive characterization.

2.1. Early Characterization

To optimize PTL structure for mass transport, factors such as pore size, distribution, porosity, and tortuosity need to be carefully considered. Various characterization techniques have been employed to analyze PTL morphology and mass transport. Earlier work by Grigoriev et al. investigated the effect of porosity by mathematically evaluating mean pore size, porosity %, gas permeability, and specific electrical resistance.[44] This study compared porosities ranging from 28–40 %, assuming spherical sintered particles in the calculations. Powder size and thickness of the PTL were measured, and an ideal geometric structure of the PTL was assumed for the theoretical correlation between porosity and electrochemical performance. The results suggested an ideal sphere diameter of between 50 to 75 μm, and optimal pore diameter of 12–13 μm. This study was instrumental in understanding the complexity of performance-structure correlations within the PTL and is heavily cited. The parameters that are used in this study (porosity, pore size) served as the baseline for the analysis of the structure of the PTL. These parameters were also used to better understand the mass transport within the PTL, commonly referred to as two-phase flow to describe the interaction between water and oxygen within the pore structure. Despite the many efforts, the theory behind two-phase flow is not well established for the PTL, and contradictions in results and conclusions do exist.[52] The discussion below highlights the major characterization techniques that contributed to the investigations of morphology of the PTL and mass transport studies.

2.2. Capillary Flow Porometry and Mercury Intrusion Porosimetry

Capillary flow porometry (CFP) is often used to study and optimize PTL porosity. Ito et al.[56,57] utilized CFP in correlation with electrochemical testing to optimize felt PTLs, evaluating porosities in the range %–75 %. The authors used these correlations to suggest that for felt structures, the ideal pore diameter is 10 μm. Current sintered PTLs have a size range of 5–30 μm.[12] As research in this area increased, CFP measurements became interchangeable with the term "wettability", especially in many recent publications, including broader electrolysis studies.[58–60]

More recently, Bromberger et al.[61] developed optimized methods to characterize the hydraulic behavior of PTLs using CFP and mercury intrusion porosimetry (MIP). CFP measures only pores that lead to continuous gas flow (channels within the PTL), whereas MIP measures both closed and open pores. A schematic of a closed vs an open pore is shown in Figure 4a. It is important to note the difference in terminology between closed and dead pores. A closed pore has one end of a channel that can reach water when flooded, and thus can be measured by MIP. The dead pores are not connected to any throats and as such cannot be measured by MIP or CFP. Using CFP, Bromberger et al. produced a schematic which illustrates gas flow rate vs. applied pressure (Figure 4b.) The scarcity of research characterizing and optimizing the PTLs prompted a 2022 paper from Nel Hydrogen and the National Renewable Energy Laboratory that introduced a standardized protocol for using CFP as a measurement for porosity in PTLs.[62] Moving forward, this protocol will aid more consistent comparisons across different publications using CFP, decreasing some of the discrepancies in the field.

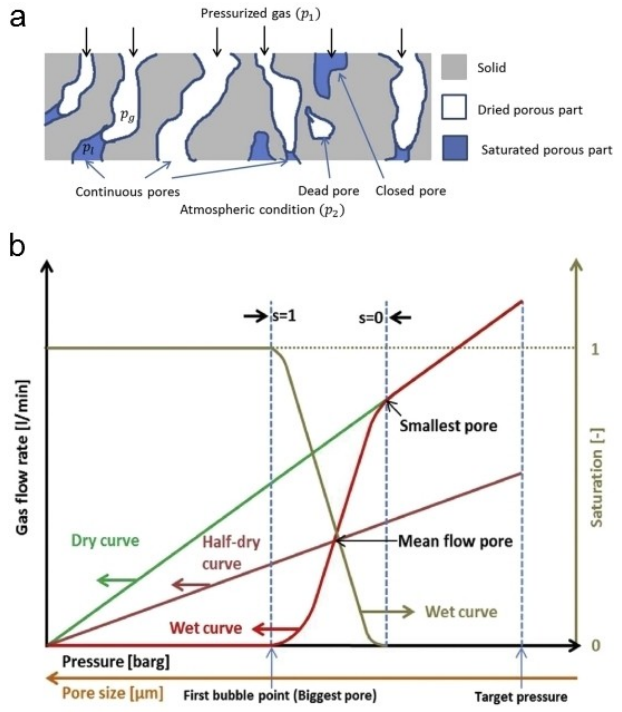

Figure 4. a) Schematic of gas flow rate vs. applied pressure with three characteristic curves of full porometry [wet curve, dry curve, and half-dry curve], and b) Schematic cross-sectional view of a partly saturated PTL.[26] Reproduced with permission from Ref. [59].

2.3. Optical Imaging

Several imaging and computational techniques were employed to study oxygen pathways and build and build-up, to optimize PTL structure for efficient oxygen removal. For example, computational fluid dynamics modeling alongside optical imaging has been used to understand flow regimes and bubble growth. In two consecutive studies by Arbabi et al. oxygen growth was characterized with help of microfluidic chips.[55,63] Simulations of the liquid-gas interface were used to better understand oxygen build up. The group introduced the terminology "critical throat", which can be used to understand dominant gas pathways and areas that are more difficult for oxygen removal.

Additional research by Dedigama et al. used a combination of optical imaging, thermal imaging, electrochemical impedance spectroscopy (EIS), and later in-situ current density mapping and optical flow visualization to analyze local current density, flow regime, and bubble formation dynamics.[64,65] Findings showed that initial bubble nucleation is dispersed, but oxygen pathways lead to the formation of much larger oxygen bubbles, which increases local current density, i.e., increases fluid transport. This is separated into the terms bubble, slug, churn, and annular flow (Figure 5). Findings from these studies were used to further understand oxygen pathway using X-ray Computed Tomography (XCT) (see section 2.6).

2.4. Neutron Radiography

Neutron radiography provides valuable information including water density gradients (known in the field as "water thickness"), and water/gas distribution (commonly referred to as "two-phase flow"). Like many techniques that are used to understand mass transport within the PTL, this technique was adopted from fuel cell research. In the early 2010's, several significant papers developed and optimized neutron radiography as a technique to understand mass transport in PEMFC systems.[66–69] This research was primarily driven by the 1996 publication from Mishima and Hibiki, which shows two phase flow modelling in capillary tubes.[70]

The first publication utilizing neutron radiography for PEMWE studies came from Selamet et al. in 2013.[71] This publication visualized two-phase transport in the PTL by simultaneously using optical imaging and neutron radiography. Water thickness and oxygen removal were measured by neutron attenuation. From this, it was shown that an increase in water flow rate can increase oxygen removal from the PTL. Additionally, it was noted that there were two types of observed oxygen bubbles. Periodic oxygen nucleation resulted in the constant growth and removal of small oxygen bubbles as

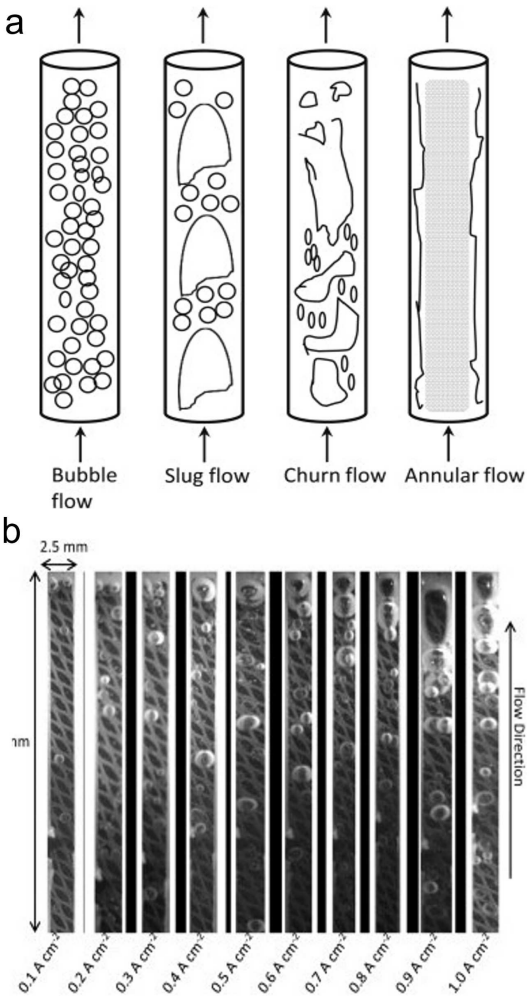

Figure 5. a) Schematic of flow regimes in a vertical channel where gas is in coexistence with liquid water, and b) flow regimes visible in the middle anode channel of a PEM water electrolyzer. Reproduced with permission from Ref. [62].

well as larger bubbles, which caused blockage of water pathways. It was noted that oxygen distribution was not uniform; water concentration at the inlet area was higher than water concentration in the outlet area.

Following this study, Seweryn et al. used neutron radiography independently to visualize the distribution of water and oxygen in the PTL.[72] This communication is broadly referenced in the literature as it proves the ability of neutrons to image water and gas in a porous titanium media. Along with significantly advancing this technique, the authors showed that water flow rate does not seem to affect water distribution, and that water saturation or water starvation does not occur. It is important to note that this work was primarily focused on technique optimization, and results were not fully realized but are heavily used by other groups that use neutron radiography to model two phase flow and analyze mass transport within the PTL.

In 2018, Panchenko et al.[73] further investigated two-phase flow in the PTL. This work reported that there is more gas under the land areas of the PTL than the channel areas of the PTL. Additionally, the authors suggested a gas-water exchange mechanism under stationary conditions, which highlighted that water to gas transport is reactive, and not continuous. This shows that as more water is supplied to the cell, more gas is produced, which can be seen by a short-term current density increase when analyzing cell performance. However, when looking at polarization curves, it is noted that the mass transport limitation seems to be caused by insufficient hydration of the membrane, known in later literature as "water starvation". Although there is a short-term increase in current density with higher water flow, this ultimately produces oxygen at a rate that does not allow proper removal from the PTL. This produces a barrier-like area where oxygen blocks water inflow from reaching the membrane. The area where PTL contacts the anodic catalyst layer is often referred to as CL-PTL interface. The oxygen barrier causes a loss of proton conductivity, which reduces cell performance. This study motivated research to optimize water removal, specifically highlighting the need for a micro-porous layer (see section 4.1).

In 2020 and 2021, several papers utilized neutron radiography to investigate two-phase flow within the PTL with the goal of improving understanding of oxygen pathways and oxygen build-up. Most of these studies use neutron radiography in combination with a complimentary technique such as x-ray computed tomography (XCT), current mapping, electrochemical testing, computational modelling, and microfluidic experiments. Findings from these publications are summarized below.

CH. Lee et al.[74] usedoperando neutron radiography to look at two phase flow in the entire PEMWE as a function of temperature from 40–80 °C. The results of this experiment demonstrated that there is a correlation between increased temperature and decreased gas distribution in the cell, which can be seen in both the anode and cathode "PTLs". Isolating the anode PTL, the study showed that as temperature increases, oxygen content decreases. This is an unexpected result, as it is known in the literature that an increased capillary number (Ca) typically decreases with increasing temperature, which would suggest an increase in gas saturation.[75] The authors suggested that this may be caused by a cell-scale phenomenon and proposed that it may be a correlation between temperature and the number of gas clusters observed in the PTL. Higher gas saturation was found under the land areas of the PTL, which confirms previous findings by Panchenko et al. Additionally, as temperature increases a higher uniformity in gas distribution is seen, and the contrast between land and channel areas becomes less significant. To further investigate this mechanism, 2D computational fluid dynamics (CFD) was used to complement radiography, confirming the hypothesis that dissolved oxygen saturation was a function of temperature. As such, the authors recommended operating PEMWE at higher temperature (80 °C), which is now standard operating temperature.

In the same year, Minnaar et al.[76] used neutron imaging and in situ current mapping to evaluate the water and gas distribution of the entire PEMWE. Specifically, this publication shows that flow field design can be altered to affect overall performance, as it can affect current density and respectively gas distribution. This work highlights the importance of looking

at the system as a whole, and not just isolating studies to evaluate the PTL. Maier et al. used a combination of neutron imaging (Figure 6), pore network modeling, and XCT to investigate two phase flow in three different PTL materials, including sintered, thick felt, and thin felt PTL.[77] Pore size distribution (PSD) was calculated with XCT results. Pore network models were also calculated based on XCT data. From this, the authors showed that water flow occurs through specific throats, which supports the concept of preferential pathways for oxygen and water in the PTL.

Literature involving neutron radiography for mass transport analysis of PTLs indicates that gas dispersion in the PTL is affected by parameters such as current density and temperature. It is also now known that oxygen content in land and channel areas is different, and that water and oxygen take preferential pathways, or specific throats, when moving through the PTL. Although this information is useful, the two-phase flow mechanism and the theory behind it are still underdeveloped areas of research. Zlobinski et al. probed further into mass transport analysis using neutron imaging with improved temporal and spatial resolution, investigating gas dispersion under a wide range of pressures and current densities in both operating and start/stop conditions.[78] The study affirmed Seweryn et al.'s findings that current density does not affect water and gas distribution.[72] Additionally, Zlobinski et al.'s work reported that between 1 and 8 bar, the gas saturation is not affected by pressure. Further, when analyzing start/stop conditions, it was found that areas within the PTL were more hydrophobic than other areas, and water re-saturation was slower due to this; it took ten minutes after stop conditions for the PTL to be fully water saturated. This result indicates that there may be areas in the PTL pore pathways that exhibit gas entrapment, which contributes to overpotential issues.[78]

Zhao et al. investigated effects of adjusting hydrophilicity of the PTL with goal of engineering the wettability of the PTL to make it super hydrophilic.[79] Treated and untreated samples were compared with electrochemical testing, operando neutron visualization, and microfluidic experiments to demonstrate that the hydrophilic PTL has better oxygen dispersion and displays lower amount of gas during operando. As a result, the electrochemical performance of the hydrophilic PTL is improved by 11% compared to untreated reference. This work highlights the importance of wettability in PTL materials that was discussed in Zlobinski et al.'s publication.

2.5. X-Ray Radiography

X-ray radiography is another technique that can be utilized for PEMWE mass transport analysis due to its ability to capture transient phenomena. As with many other methods, this technique was first used and developed for PEMFCs research. Manke et al. published a study in 2007 which used radiography to track water evolution and transport in fuel cells.[80] Several other ex situ studies from the early 2010's further developed this technique to learn more about the microstructure and water transport in fuel cells.[81–83]

These developments enabled a breakthrough 2015 study by Hoeh et al., that reported operando x-ray radiography investigation of PEMWEs.[84] This publication describes issues with techniques such as neuron radiography (Figure 7) and optical imaging, that include lack of the spatial and temporal resolution that is desired to thoroughly investigate the mass transport phenomena. In-situ synchrotron X-ray radiography (SR) mitigates some of these issues to better understand the two-phase flow phenomena; specifically, the gas discharge from the PTL into the flow channels. The authors looked at frequency of

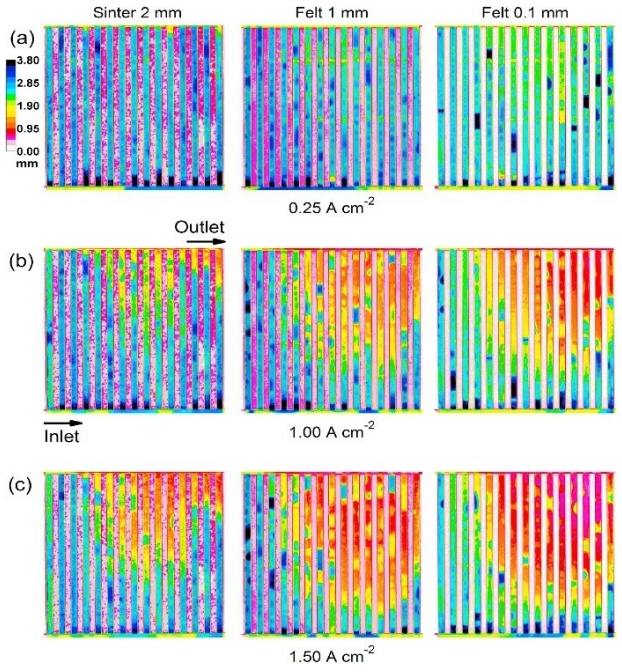

Figure 6. Neutron radiographs at a current density of (a) 0.25 A cm^2, (b) 1.00 A cm^2, and (c) 1.50 A/cm. Reproduced with permission from Ref. [75].

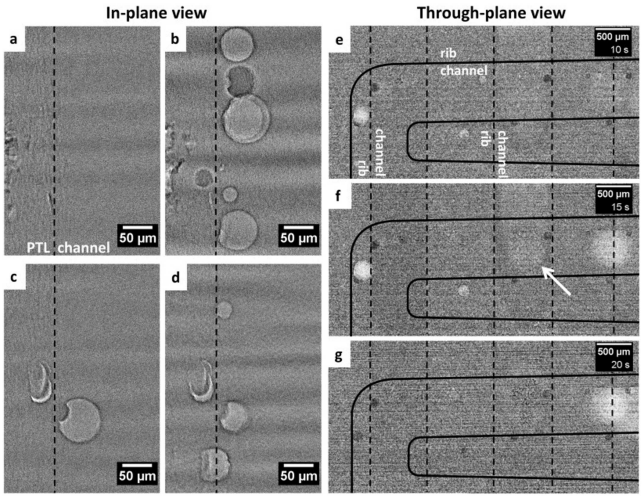

Figure 7. a–d) Visualization of the increase in number of discharge sites along the PTL-cathode channel interface, e–g) visualization of gas transport in the anode (solid line) and cathode channels (dashed line). Reproduced with permission from Ref. [82].

discharge volumes and derived occurrences of selective gas transport pathways. Additionally, the publication showed that more gas pathways occur at higher current density. This indicates that water saturation of the PTL can be manipulated by current density. Authors state that the addition of this technique to mass transport analysis should help future cell and PTL design to facilitate more efficient gas removal from the PEMWEs.

The results of Hoeh et al.'s publication have shown the significance of using x-ray radiography as a tool to measure oxygen discharge frequency and observe selective oxygen pathways. Unfortunately, this technique is limited to two-dimensional analysis. As such, it is best to be used as a complimentary technique to other methods employed in mass transport studies. Leonard et al.[85,86] used X-ray Radiography in combination with X-ray Computed Tomography (XCT) in two consecutive studies that focus on the complexity of visualizing mass transport in the PTL. Although the XCT in these studies cannot capture variation between gas and liquid in the PTL, the addition of SR provided a fuller understanding of the layer in operando conditions.

2.6. X-ray Computed Tomography

XCT, also known as X-ray tomographic microscopy (XTM), is a powerful technique for the structural analysis of the PTLs. Micro-XCT is commonly used interchangeably with the term high-resolution CT. This technique has spatial resolution on the micron size[87] and can be conducted with both laboratory-based and synchrotron-based instruments to provide pore size, pore size distribution, tortuosity, in-plane porosity, and through-plane porosity of PTLs. These parameters in correlation with electrochemical testing or two-phase flow visualization provide a greater understanding of where blocks in cell efficiency occur. Nano-XCT, which can analyze material on the sub-micron, down to tens of nanometer scale, has also been utilized for PEMWEs characterization, but the primary use of it is analysis of CLs.

The XCT's ability to differentiate materials based on X-ray attenuation has been widely utilized for fuel cell development, and in the mid 2010's was applied to analyze PEMWEs. Initial PTL analysis using XCT focused on the morphology or structure of the PTLs. It is important to note that XCT of PEMWEs is more difficult because PEMWEs use titanium PTLs as a material in replacement of the carbon employed in fuel cells. Specifically, the high x-ray attenuation of titanium produces artifacts in the reconstructed images, and an effort to correctly remove these has become imperative.

In 2014, Zielke et al.[88] used laboratory based XCT to study the morphology of eight different fiber PTL materials, referred to in the paper as current collectors, comparing their thermal conductivity, porosity, water permeability, and electrical conductivity. This paper contributes heavily to the initial understanding of pore size distribution (PSD) within the sintered and fiber PTL. With many parameters to analyze, this paper acknowledged the complexity of high degree of freedom analysis when correlating the PTL structure with performance. Two correlations that stand true with both fiber and sintered PTLs were demonstrated. There is an exponential correlation between porosity and two phase (water and titanium) thermal conductivity, as well as the correlation between electrical conductivity and water permeability. These findings can be used in future work to reduce the degrees of freedom in models when correlating PTL morphological parameters to performance parameters and testing.

Suermann et al.[31] evaluated three different sintered PTL materials, with varying bottleneck pore sizes of 5, 10, and 20 μm. XCT data was used to calculate porosity, pore size distribution, and particle size distribution. PTL structure was compared to a variety of current densities, temperatures, and pressures to better understand correlations between structural parameters and mass transport overpotentials. Two important correlations between structure and performance were shown. High frequency resistance (HFR) is higher in the large pore material. This does not correlate with bulk electrical conductivity of the PTLs, indicating the issue arises with ICR at the catalyst layer-PTL interface due to larger particle sizes. Additionally, large particle size was associated with higher mass transport overpotential. The authors suggested that a more detailed understanding of CL-PTL interface is needed to interpret this result. The interface between CL and PTL has been heavily researched and will be discussed in more detail in later sections.

Following this work, several studies further contributed to the current understanding of the correlation to PTL structure and PEMWE performance. Majasan et al. published consecutive papers in 2018 and 2019. The 2018 study compared two sintered PTLs with significantly different pore sizes.[89] A large pore PTL (LP-PTL) and small pore PTL (SP-PTL) were analyzed with XCT (Figure 8). The SP-PTL outperformed the LP PTL; ohmic resistance was significantly better with the SP-PTL and mass transport resistance was comparable with both PTL's. These results support Suermann et al.'s statement that the ICR at the CL-PTL interface plays a significant role in PEMWE performance and must be further explored. The 2019 study by Majasan et al. evaluated four different sintered PTLs varying in pore size.[90] The results agreed with the previous study; further reaffirming that to decrease overpotential in the PEMWE, contact between the CL and the PTL should be maximized.

Schuler et al. visualized six different PTL's of varying porosity and fiber thicknesses, comparing structural parameters with electrochemical performance results in two consecutive papers.[91,92] This work differs from previous reports as it focused on felt PTL materials and compared these to a standard sintered PTL; both materials are used in industrial PEMWE applications. Additionally, recognizing the importance of the CL-PTL interface, surface roughness of these PTLs was analyzed. Combined results from these papers indicate that the fiber PTLs have better transport properties than the sintered material. However, the sintered material has better thermal conductivity due to its smaller porosity. Permeability and diffusivity do not show correlations to performance testing results. Authors hypothesized that as long as they are above the threshold, these two

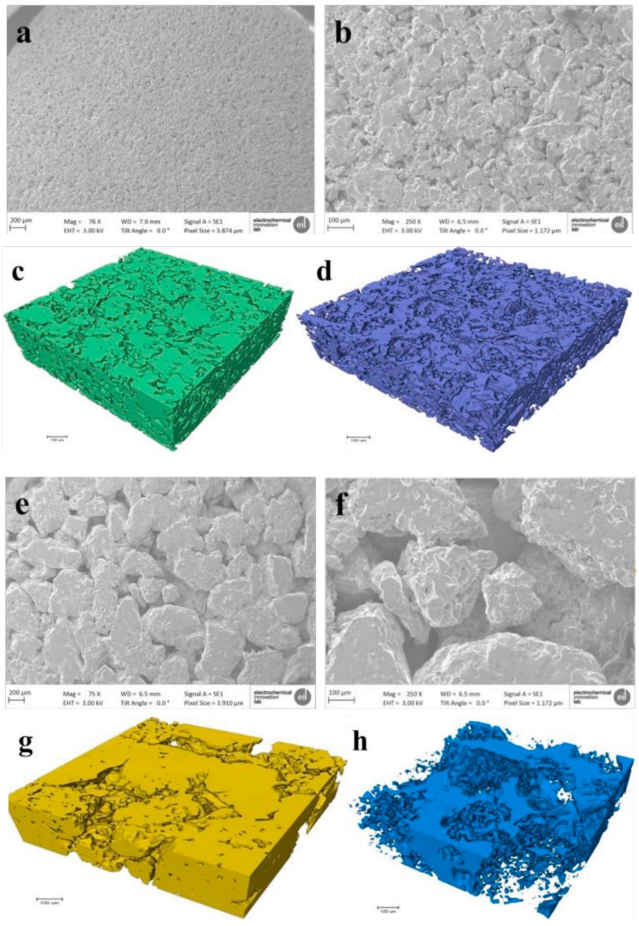

Figure 8. Morphology and 3D structure of PTLs. SP PTL for a) low magnification SEM b) high magnification SEM c) XCT reconstruction of solid material d) XCT reconstruction of pore network. LP PTL for e) low magnification SEM f) high magnification SEM g) XCT reconstruction of solid material h) XCT reconstruction of pore network. Reproduced with permission from Ref. [88].

parameters are not limiting factors for overpotential issues; these thresholds are currently unknown and need to be further investigated. Similarly, throat size in the fiber PTL does not seem to be limiting performance in these PTLs, where the smallest pore size average is ~14 μm. Presumably, this is because pores are significantly larger than in sintered materials; more research needs to be done to see when throat sizes start to drive mass transport limitations.

In 2021, Pushkarev et al.[93] published a study looking at catalyst coated PTL performance on two different sintered PTLs that varied in pore size. This study used a combination of characterization techniques including XCT, CFP, scanning electron microscopy (SEM), and MIP to correlate PEMWE structure to performance, highlighting importance of PTL structure. Ohmic and activation overpotentials were not significantly affected by the difference in bulk PTL structure. Mass transport overpotentials were found to be dependent on PTL structure, especially at higher current densities; higher porosity and lower tortuosity allows oxygen to leave the system more efficiently. These results echo previous findings in the literature. Adding to this, the study analyzed cathode GDL in combination with the anode PTL, which provided further insights to overall PEMWE performance by showing that decreasing porosity on the cathode GDL can contribute to recovering overall voltage loss. Studies of cathode porosity are scarce, and these initial results require further investigation. Peng et al. investigated five different Ti mesh PTLs varying in porosity.[94] XCT is used to calculate porosity, mean pore size, through-plane tortuosity, in-plane tortuosity, and PTL thickness. These parameters were then related to polarization curves. In this study, a low Ir loaded catalyst (0.05 mg_{Ir}/cm^2) was used in the PEMWE stack. Notably, at low Ir loadings, performance results are largely dependent on the PTL properties.

In 2022, Weber et al.[95] visualized five felt PTLs varying in thickness ranging from 0.16 mm to 2 mm with XCT. The goal of this study was to identify how thin the PTL can be to reduce manufacturing and material costs, while still providing optimized efficiency. Samples were tested electrochemically, and overpotential breakdowns were analyzed. These PTLs have similar structural parameters excluding overall thickness, therefore clear conclusions can be made by directly comparing thickness to overpotential. Results show that ohmic overpotential slightly increased as PTL thickness decreases. It has been hypothesized that this is due to slightly lower heat transfer resistance. Mass transport overpotential decreases when comparing the 2 mm PTL to the 0.5 PTL; authors suggested that this decrease is due to the shorter transport pathways from the CL to the BPP flow field. Additionally, as PTL thickness is decreased from 0.25 mm to 0.16 mm, the mass transport overpotential increased again, most likely due to CL water starvation, which is in line with modelling results from Chen et al.[96] As such, authors hypothesize that an ideal PTL thickness is a ratio of BPP/FF land width and PTL thickness of 0.5 for felt PTLs. This new ratio is introduced as a parameter ΦTP/IP, which authors encourage researchers to consider when optimizing the PEMWE cell.

As can be seen, XCT characterization has been primarily used for structural analysis of the PTLs. Initially, mass transport via XCT was not analyzed due to the high x-ray attenuation of titanium and limitations of operando studies due to long scan times. Recent developments allowed for shorter scan times, which prompted operando XCT studies. Two important publications by the Zenyuk group reported development of operando XCT for the analysis of two-phase flow.[85,97] A 2018 paper by Leonard et al. investigated mass transport with operando synchrotron XCT by substituting the titanium PTL material with a short-term carbon felt based replacement.[85] XCT results combined with x-ray radiography analysis allowed XCT to successfully analyze mass transport in a functioning PEMWE cell. XCT analysis showed catalyst dissolution and redeposition into the PTL over time, with more catalyst thinning and redeposition occurring at higher current densities. X-ray radiography tracks bubble residence and bubble detachment times in relation to current density, which can be used to better understand gas transport mechanisms in the PTL.

A 2020 study by Satjaritanun et al. uses operando XCT without the reliance on neutron imaging as a secondary

technique.[97] This study also used a carbon-felt replacement instead of the titanium PTL and XCT images were coupled with CFD calculations to better understand oxygen dispersion in the PTL under operando conditions (Figure 9). This study found that oxygen forms preferential pathways, which confirms results found in previous radiography studies. Additionally, it was noted that oxygen seems to form in higher concentrations periodically, which authors hypothesize is due to the difference in in-plane and through-plane tortuosity, which permits oxygen to merge as a periodic waveform. This work suggested that tailoring the PTL by pore size and wettability would allow for better oxygen removal from the PTL, encouraging the implementation of a gradient like PTL.

Contributing to the studies of mass transfer with XCT, De Angelis et al.[98] reported operando investigation that used a staining agent to enable identification and differentiation of water and oxygen in XCT within the titanium PTL. The results of this work show that within the PTL during operation, both stable and unstable oxygen pathways occur, with the unstable pathways evolving to transient bubbly flow regime with increased current densities. Oxygen instability (disrupted pathways) reside under the channel areas of the PTL, where stable pathways occur under the land areas of the PTL. Oxygen tends to occupy larger pores in the PTL network where water will occupy smaller pores. Following results from Satjaritanun et al, it is observed that distinct oxygen cluster sites decrease with increased current density, as large in-plane bridges form to make larger oxygen clusters, or pathways. Additionally, the authors identified capillary-driven flow regimes for all analyzed current densities. This allows the conclusion that oxygen flow is only determined by the PTL morphology. As such, the structural adjustment of the PTL such as the implementation of a gradient like PTL or the introduction of an anisotropic structure within the PTL could mitigate oxygen build up and sluggish mass transport within the PTL.

3. Protective Coatings and their Characterization

Currently, Pt is used as the state-of-the-art protective layer for the PTLs, but other PGM materials including Au have been investigated. Recently, research has been conducted to reduce the loading of PGM materials by creating thin PGM coatings, replacing PGM coatings with non-PGM alternatives, and through various post-treatments to modify the chemistry or morphology of the PTL. Various characterization methods have been employed to evaluate PTL protective coatings. The main characterization techniques for coating analysis can be split into four categories: electrochemical characterization, morphological characterization, elemental characterization, and chemical characterization. Electrochemical characterization heavily utilizes cyclic voltammetry (CV), potential sweep voltammetry (PSV), EIS, and stability testing. Morphological characterization uses SEM, transmission electron microscopy, scanning transmission electron microscopy (TEM/STEM), and XCT. Elemental characterization includes energy-dispersive X-ray spectroscopy (EDS) and inductively coupled plasma mass spectrometry (ICP-MS). Chemical analysis includes gravimetric analysis, X-ray diffraction analysis (XRD), Auger electron spectroscopy (AES), X-ray photoelectron spectroscopy (XPS), and time-of-flight secondary ion mass spectrometry (ToF SIMS). These techniques offer insights into coating composition, morphology, and degradation mechanisms, but every technique provides different information, each with its own advantages and disadvantages. This is particularly important in chemical analysis since each technique varies in multiple parameters, such as depth of analysis (bulk vs surface), spatial resolution, and analysis area. Consistency in characterization methods and long-term durability testing are essential to making informed decisions about suitable coating materials for PTLs moving forward. Detailed summaries of different coating approaches and their related characterizations are detailed in the following sections.

It should be noted that as the main goal of these protective coatings is the stability of the PTL, stability or degradation testing is typically prioritized in results. The stability of the component can be characterized in several ways. Most commonly electrochemical testing, often long-term operation testing, is reported. In addition to long-term operation testing, polarization curves and EIS are often collected at different intervals. Furthermore, accelerated stress testing is used to understand extreme degradation. In addition to electrochemical testing, physical characterization techniques as listed above are utilized when correlating materials properties and their stability and degradation.

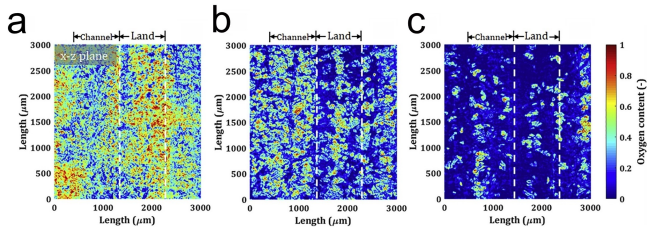

Figure 9. Top-down comparison of oxygen content within the different portions of the PTL. a) x-z plane at the CL and PTL interface. b) x-z plane in the middle PTL portion. c) x-z plane at the PTL and channel interface. Reproduced with permission from Ref. [96].

3.1. PGM-based Coatings

Initial investigations of Ti material replacements and Ti protective coatings have been conducted with bi-polar plates (BPPs). BPP is also a titanium-based layer that passivates under the condition of the cell. The BPP is a large flat material and as such, is considered a simpler system to study than the PTLs that have more complex morphology. To reduce overall cost of the PEMWEs, materials like copper[99] and stainless steel (SS) have been investigated as alternatives to Ti. A different approach is to coat the BPP or PTL with a protective coating, typically a PGM material like Pt of Au. More recently nitride and oxide coatings including TiN[100], NbN[101], and Ti_4O_7[102] have been

investigated for both the classic Ti BPP and the alternative SS BPPs.

In an initial study by Jung et al. in 2010, BPPs coated with Pt were compared to the unprotected titanium BPP materials under operating conditions of the cell (2.0 V) showing significant performance improvements of the material with coating.[103] In 2016 Rakousky et al investigated a 200 nm platinum layer that was chamber sputtered onto a sintered Ti-PTL material.[104] The protected PTL was compared to the unprotected Ti PTL under the same PEMWE testing conditions of 2 A/cm^2, at 80 °C for 1000 hours. The degradation rate of the Pt-coated PTL was reduced by approximately 89 %, proving that a protective coating can significantly improve the performance of the PTL and thus the overall PEMWE. This study is indisputably an advancement in the PTL and PEMWE field, but it is important to note that the thickness of the platinum layer was estimated based on sputter chamber parameters and not measured with appropriate methods such as TEM. As such, the consistency of coverage and thickness of the Pt coating before or after electrochemical testing are not known, leaving gaps in the understanding of the efficiency of the expensive PGM group metal coating.

In a continuation of this research two years later Rakousky et al. analyzed the degradation of Pt-protected PTLs.[105] The study uses an accelerated stress test (AST) by increasing both the amplitude (3.0 A) and operating time (1940 hours) of a PEMWE stack cell to understand the degradation of a Pt-protected PTL. Polarization curves showed decreased cell performance at later operating times and EIS indicated ohmic resistance increases and mass transport losses over time. This paper also uses only very limited physicochemical characterizations to complement electrochemical measurements. SEM was employed to measure the thickness of Pt coating before electrochemical testing (Figure 10). Note that the morphologically bumpy sintered PTL coated with Pt by sputtering produced an unevenly coated Pt layer, although full coverage of the PTL was observed. After cell operation was terminated, the cell was disassembled to isolate the PTL. It was found that the Pt protective coating detached from the PTL and adhered to the anode coating. This factor was indicated as the main reason for the degradation measured with electrochemical analysis. This further highlights the importance of visualizing coatings pre- and post-testing to identify degradation mechanisms.

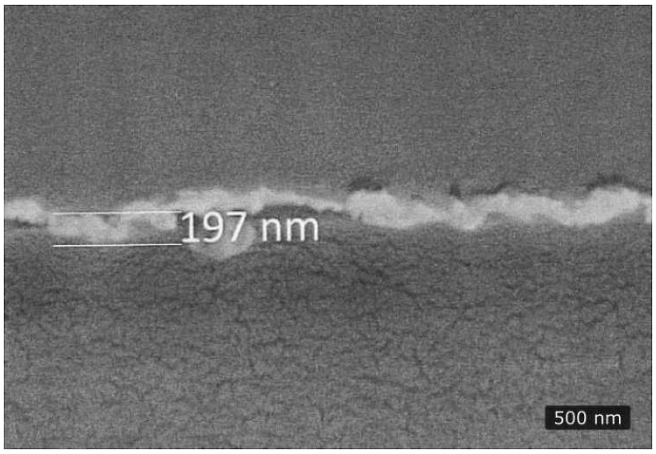

Figure 10. FIB-SEM Image of Pt coating on PTL. Reproduced with permission from Ref. [105].

Kang et al. investigated a gold (Au) protective coating applied to circular pore-shaped flat titanium sheets as potential PTL material.[106] Unlike the conventional sintered or felt PTL materials, this material had manufactured circular, homogenously distributed and sized pores. A series of these PTL-like materials were coated with Au using a variety of techniques, including electroplating and sputtering, producing coatings with different thicknesses. The electrochemical results (EIS, polarization) indicated improved performance of electroplated Au samples in comparison to uncoated and sputtered materials. The materials were analyzed with SEM, revealing that electroplating gives a more homogenous coating at multiple thicknesses. EDS spectra showed less intense Ti peaks in the electroplated samples, confirming the electroplated sample has a more even distribution and coverage of Au than the sputtered coating. EIS analysis showed that 180 and 820 nm thick electroplated Au coatings resulted in similar performance, indicating that even 180 nm of Au coating was sufficient to reduce Ti oxidation of the layer during operation. It is important to note that these results were not compared to the commercial PTL materials or other more commonly explored Pt coatings. Additionally, these samples were not studied following AST and didn't include postmortem electron microscopy characterization. This makes comparisons with previous studies involving Pt coatings difficult.

3.2. Alternative Non-PGM-based Coatings and PTLs

The cost associated with PGM-based coatings and Ti-based PTLs motivated research to find alternative more cost-efficient materials to replace both the PGM protective coating and the commercially used Ti-PTLs. Daudt et al. proposed using a Niobium Nitrate (NbN) protective coating on Ti-PTL to reduce the Pt use in the PEMWEs.[107] This was considered based on similar work that was conducted to reduce cost of BPPs protective coatings.[108,109] Electrochemical results (CV, polarization) from this study indicated that in short term operation, the NbN coating improved performance and decreased titanium oxidation. PTL coating microstructure and coating thickness of freshly produced and tested samples were analyzed by SEM, and phase composition was determined by XRD. Conductive probe atomic force microscopy (CP-AFM) was used to generate current images of the coated and uncoated PTL before and after electrochemical testing to confirm conductivity losses in post-mortem samples. Although results of this work indicate that NbN coatings may be a promising alternative to Pt- or other PGM-based coatings, no long term or AST testing was conducted on these samples, limiting impact of the study. Additionally, electrochemical testing was conducted on the PTL material by a three-electrode electrochemical cell, not in the PEMWE cell, which could skew interpretation of results.

The most notable alternative to titanium PTL is SS. However, it has been shown that SS PTLs may lead to ion poisoning which promotes membrane degradation under the conditions of the cell if unprotected. This motivated investigations of protective coatings.[110–112] Some evidence was provided that coating the SS PTL with a layer of Ti or a different protective coating allows similar short term electrochemical performances. However, the long-term durability of this material has not yet been investigated. Additionally, potential degradation due to hydrogen embrittlement which is known to easily occur in SS is of concern. Stiber et al.[113] investigated a SS based PTL that was coated with a thin layer of Ti, followed by a thin layer of Nb/Ti. Electrochemical results showed that while maintaining the same performance, current density can be increased by over a factor of 10. This is a promising indication of the possibility of transitioning from Ti to SS materials. This study utilized extensive characterization to better understand the coating and its properties. Samples were cross sectioned and analyzed with SEM/EDS to study initial elemental distribution and coating purity (important for corrosion resistance), coating thickness and homogeneity, and contact between the SS PTL and the coating. As the SS PTL material will act differently than the typical Ti-based sintered/felt PTL, MIP and XCT were used to understand porosity and pore size distribution, coupled with pore network modeling (PNM) to analyze mass transport. Additionally, ICR testing between coated SS PTL and the CL was conducted to evaluate effect of coating on the OER rate. XPS and ICP-MS were also used to investigate corrosion resistance by tracking any Fe leeching. Results of AST and correlated characterization show no evidence of SS corrosion on the coated sample and demonstrate performance competitive with commercially used PTL materials. Additionally, the PNM work showed increased mass transport efficiency in the SS material in comparison to typical Ti PTL materials. The results of this study show promise for the replacement of Ti based PTL materials in future generations of the PEMWE stack. This study also presented a more comprehensive characterization in comparison to other reports. By utilizing multiple techniques to analyze materials, a much deeper understanding can be achieved due to the unique information each technique provides. This is especially valuable for investigations of novel materials.

Recent studies investigating potential BPP replacement materials have shown evidence for decoupling of the BPP from the highly acidic polarized environment near the anode CL due to the high resistivity of the PTL near the CL. Becker et al. presented evidence that most polarization of the PTL occurs near or at the interface of the CL, causing a decoupling effect between the CL/PTL interface and the BPP/PTL interface.[114] After reporting this result, Becker et al. suggested using a carbon coated SS based PTL material for the bulk of the anodic PTL, followed by a the classic Ti/Pt protective coated material that is in contact with the CL.[115] The follow-up study further studied the practicality of this suggestion by investigating the electrochemical potential throughout the thickness of the PTL and the spatial profile of the PTL using a combination of modeling and open circuit potential testing (OCP) and ex situ corrosion testing to better understand the decoupling effect. Using modeling and XCT measurements, the group predicted that the corrosion of the SS PTL would only affect the 200 μm of material that is closest to the anodic CL, where most commercial sintered Ti/Pt PTLs are around 1100 um. This thickness was used in the newly proposed combined SS/Ti/Pt PTL material. Electrochemical results paired nicely with computational results; no changes were seen during a 30-day stability test. The combined results indicate that deeper than 200 μm into the PTL, the local potential experienced was much lower, suggesting that this proposed model might be feasible. It is stated that SEM-EDS analysis was conducted to analyze as-received and tested samples, but these results are only briefly shown and discussed in the S.I. This study also utilizes AES and ICP-MS for postmortem analysis to identify changes in the chemical states and contaminations. Results of this analysis showed degradation of the carbon coating, but only small changes to SS components, indicating the potential for this model to be used as a replacement for Ti/Pt PTL materials. This work shows potential for replacing commercially used Ti-based PTL materials with SS alternatives. However, further studies of scalability, cost analysis, and longer durability testing are needed before the PEMWE research and industrial community can decide on the practicality of SS as PTL material in commercial applications.

3.3. Post-Treatments of PTLs and Protective Coatings

An alternative approach to reducing passivation on the titanium PTL is to treat the surface of the titanium to alter its composition and/or morphology. Bystron et al.'s 2018 study acid etched Ti PTL to remove the passivated TiO_x layer.[116] This treatment was followed by an HCl treatment which effectively changed the titanium surface composition from TiO_x to a titanium hydride species, TiH_x. Although hydride chemical analysis is difficult, this paper pairs bulk (XRD), surface (XPS), and morphological (SEM) analysis to identify and study the formation of surface hydrides on the treated PTLs.[117] The shift in the XPS Ti 2p and O 1s binding energies showed clear evidence of the surface composition changes when comparing pre-etched, etched, and aged samples. Authors suggest that this supports evidence of TiH_x formation and subsequent re-formation of the thin oxide layer post-aging. Subsequent electrochemical testing showed short-term evidence of improved performance over pristine PTL materials. As per previous coating techniques, further investigation of the long-term performance and degradation of this treatment is needed. This is particularly important considering the potential negative effects of hydride formation, specifically hydrogen embrittlement.

Bystron et al.'s use of acid etching prompted Bautkinova et al. to investigate etching and subsequent coating the PTL with a PGM protective material.[118] With the addition of coating, identifying oxides and hydrides becomes even more difficult as these are now buried within the material. XRD was used before the deposition of a protective Ir-coating to confirm phase composition. Temperature programmed desorption (TPD) was

also employed to identify conditions where hydrogen embrittlement occurs, and SEM/EDS was used to track changes in morphology and understand coating homogeneity. Approaches like XPS which could previously be used to track titanium hydrides and oxides are no longer suitable as these layers exist below the top surface of the material. As such, a lack of knowledge exists in understanding the existence and evolution of oxides and hydrides under the conditions of the cell for these complex materials. The development of better approaches for characterization of buried layers and identification of both oxides and hydrides is needed.

3.4. Thin PGM-based Coatings

Some research groups have focused on using smaller amounts of PGMs to produce thin coatings, instead of replacing PGM coatings with less expansive alternatives. As previously discussed, to maintain long term stability as a protective coating both Pt and Au require a thick coating of around 200 nm. Lui et al.[119] proposed using Ir as a protective coating in place of Pt or Au. The basis for this idea is to utilize the higher electrical conductivity of IrO_2 in comparison to gold or platinum oxides to allow long-term stability with a thinner protective layer. The initial study showed evidence that a thin Ir coating decreases ohmic resistance in comparison to uncoated PTLs. Kang et al. later confirmed this finding.[35] In addition to electrochemical testing, Lui et al utilized gravimetric analysis, FIB-SEM and nano-XCT to characterize the coatings.[119] Gravimetric analysis was used to calculate Iridium loadings. Top-down SEM and nano-XCT confirmed that the Ir is distributed homogeneously spatially throughout the thickness of the PTL, and FIB-SEM provided thickness measurements estimating coatings to range from 20 to 150 nm. While these techniques provided useful information, some information, such as understanding buried oxide is lacking. More information on whether the protective layer is properly mitigating the formation of TiO_2 is needed.

In a follow-up study, Liu et al.[120] conducted a more in-depth analysis of Ir coatings, comparing Ir to Pt and Au protective coatings correlating electrochemical analysis and surface characterization. The results of this study indicated that Ir coatings mimicked the performance results of the state-of-the-art Pt coating and outperformed the Au coating (Figure 11a). XPS was used to better identify oxidation states at the surface of the material (Figure 11b). This study also introduced ToF SIMS as a characterization technique to track coatings, bulk PTL material and the interface between them (Figure 11c). ToF SIMS is widely used to study coatings and buried interfaces of various materials for other applications, where the material is a flat substrate. Despite more complex morphology of the PTLs, ToF SIMS provided useful information about differences in elemental composition and chemical species throughout the depth of the different coatings. It also identified the presence of oxides at the interface; the formation of oxide associated with both coating and oxide associated with Ti PTL were observed. This study highlights the importance of multi-technique analysis when dealing with complex materials and buried interfaces. It also motivates further optimization of ToF SIMS for these morphologically complex materials to enable a more thorough understanding of the coated or modified PTLs and their degradation.

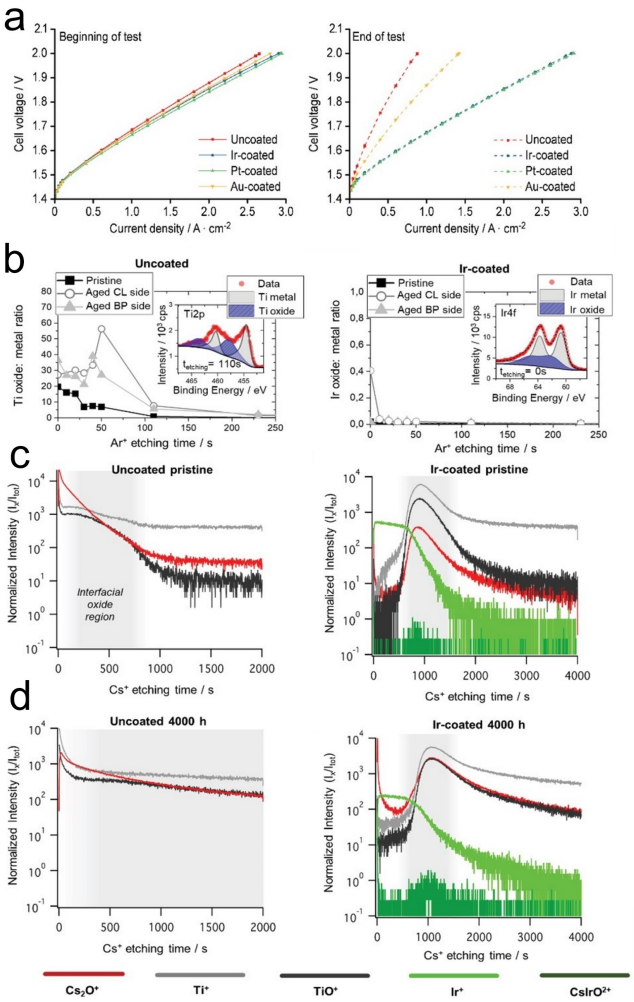

Figure 11. a) Electrochemical testing b) XPS and c) ToF SIMS analysis of uncoated and Ir coated PTLs. Reproduced with permission from Ref. [119].

4. PTL/CL Interface Optimizations and Characterization

Several strategies and techniques have been examined to optimize the interface between the CL and PTL. A common strategy involves implementing spatially graded PTLs . Research conclusively shows that the spatially graded PTLs improve overall cell efficiency due to enhanced oxygen removal and better PTL/CL interfacial contact, but scale-up approaches for these materials must still be further studied. The second direction is investigations of porous transport electrodes (PTEs). This work was motivated by studies of traditional CCM based systems that correlated electrochemical results with SEM, EDS, and XPS to better understand the PTL/CL interface. As with

protective coating studies, a priority for testing is to understand the stability of these components. Results of these studies show major degradation of the MEA, specifically identifying that areas of non-contact between the PTL and CCM exist, influencing performance. Several approaches to directly coating PTLs with catalysts and protective materials have been investigated. Traditional catalysts including Ir and Pt, as well as novel catalysts, have been used and variations in fabrication methods and structural properties have been explored. Electrochemical characterization and physical analysis through techniques like XRD, SEM, and TEM have been used to assess the performance, stability, and morphology of PTEs.

4.1. Development of the Gradient PTLs and MPL

Results of mass transport and structural correlation studies discussed in the introductory PTL section are challenging to compare across due to the significant variation in parameters from one experiment to another and one material to another. Even so, it is clear from the two-phase flow results that structural changes in the PTL that vary porosity in a gradient-like manner could decrease the overpotential issues caused by preferential oxygen pathways. Two phase flow and electrochemical findings motivated studies involving PTLs with gradient porosity or introduction of micro porous layer (MPL). MPL is a lower-porosity titanium material that is attached to the regular PTL structure, at the interface with the CL.

J.K Lee et al. reported the development of a spatially graded PTL to mitigate oxygen barriers.[121] This custom PTL was developed with vacuum plasma spraying, which allowed to produce areas on PTL with high porosity (HP) and low porosity (LP). Operando neutron radiography analysis showed that oxygen saturation is significantly reduced when the CL is next to the low porosity side of the graded PTL. The pore networking modeling confirmed the neutron radiography results. Additionally, electrochemical results showed an increase in performance with this orientation, which the authors inferred was related to better oxygen removal from the PTL. It was suggested that the low porosity allowed for more contact points with the CL, which contributed to better electron conductivity. Indeed, lower HFR and mass transport overpotentials were observed with the LP to HP configuration. This is one of the first results indicating that the gradient PTL, which had been mentioned in previous studies, could be beneficial to the optimization of the PEMWE.

Schuler et al. produced three MPLs with varying particle size ranging from 2–20 μm (Figure 12).[122] Results show that the smaller MPL particle sizes, determined with XCT, slightly decreased mass transport overpotentials, and all ML-PTL's had increased catalyst utilization in comparison to the original PTL. In a collaborative study by Zlobinski et al., the authors looked at the same set of MPLs with operando neutron radiography.[123] This study evaluated gas dispersion of the ML-PTL structures as well as the bare PTL at a wide range of current densities (.1–4 A/cm^2) and pressures (1–8 bar). Results showed that with all ML-PTLs, there is an increase in water saturation in the MPL section, and an increase in oxygen saturation in the more

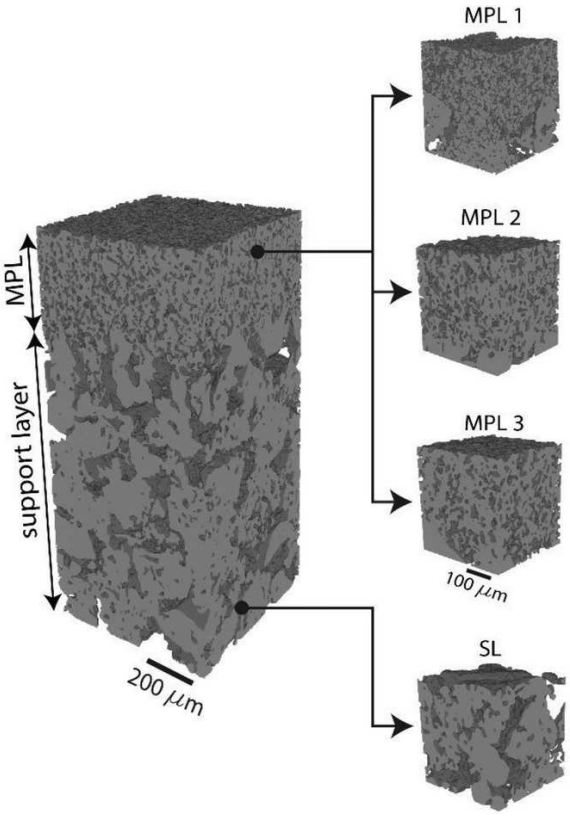

Figure 12. XCT 3D reconstruction highlighting different MPL particle sizes. Reproduced with permission from Ref. [121].

porous PTL section. The decrease in the pore size in the PTL to give thinner porous pathways, results in an exaggeration of the results. Specifically, the smallest particle MPL (6 μm particle size) had significantly fewer oxygen barriers. Kang et al. published two back-to-back studies that further explore the addition of the MPL. Specifically, they investigated MPLs made with 5 μm irregular titanium particles as well as titanium sheets with spherical pores of about 30 μm. In both cases, the addition of the MPL reduced the HFR, increasing catalyst utilization.[124,125] Stiber et al. reported a new PTL structure that combines a sintered titanium material with a mesh material via diffusion bonding, mitigating the reliance on the BPP.[126] This led to an increased operating range because of better oxygen removal from the system. Kim et al. introduced a bi-layer mesh Ti PTLs with varying pore sizes.[127] Finite element analysis (FEA) was utilized to understand the contact at the interface between the CL and the PTL. Results showed reduced ohmic losses with this material in comparison to commercially available PTLs due to the increased interfacial contact at the PTL/CL interface.

The above findings highlight the positive impact of the incorporation of a graded PTL. Although many results demonstrate improvement, some gaps in knowledge exist, specifically with mass transport mechanisms within graded PTLs. Ideally, future investigations should analyze mass transport at the CL and CL/PTL and correlate those results to performance characteristics to better understand the CL/PTL interface. This analysis is currently limited due to spatial and temporal resolutions of

imaging techniques in the field, specifically with neutron radiology. A recent study by Nakajima et al. mitigates this limitation with combined numerical modeling and EIS to investigate an MPL with an interdigitated flow field.[128] The results of this study highlight that modeling can add significant insight in studies where physical characterization approaches lack. Even so, scale-up approaches on a graded PTL will need to be investigated before it is widely utilized and commercialized.

4.2. Investigation of the PTL/CL Interface in CCMs

Major investigations of the interface between the PTL and the CL started in 2020 alongside the development of the MPL. As previously discussed, HFR was found to increase with increasing PTL pore size.[31] Since bulk properties do appear to affect these results, it is suggested that the interfacial contact resistance (ICR) between the CL and the PTL is the driving factor for this result.[31] In 2020, Lopata et al. studied the interface of the CCM and PTL as a function of PTL pore size and catalyst loading.[129] This study evaluated HFR, oxygen bubble coverage and ionomer conductivity and concluded that with decreasing catalyst loadings, the PTL properties (pore and grain size) become increasingly significant to transport limitations within the cell. Additionally, bulk PTL properties like average porosity and permeability did not greatly affect results, highlighting that the interface between the PTL and CL is driving limitations within the cell. In this study, only electrochemical results are shown. Although this study provided important insights, the contact between the CCM and PTL must be visually characterized to better understand where and how contact issues occur between the layers.

A recent study by Kwen et al. correlated electrochemical results with SEM-EDS and XPS to better understand interfacial contact of the PTL and the CCM.[130] The operating conditions of the PEMWE cell were adjusted to reduce IrO_x to metallic Ir in areas where ionic and electrical conductivity between the CCM and PTL are active. SEM-EDS used to visualize oxygen on the deconstructed CCM, highlighting areas where IrO_x still remains due to a lack of electrical and ionic conductivity between the PTL and CCM. XPS analysis confirmed partial conversion of IrO_x to a combination of Ir and IrO_x, verifying EDS results. The large areas of non-contact between the felt PTL and the CCM in this study were not surprising, since this study was published after reports that indicated that sintered or MPL layer connection increases conductivity with the CL. However, analysis of the SEM showed that the interfacial connection under the "land" vs "channel" of the flow field differ- while both areas have evidence of contact and non-contact areas, the non-contact areas under the land have more extreme issues with electrical conductivity. This is supported by SEM imaging, where cracks in the CCM are more evident in non-contact areas under the land (Figure 13). The authors suggested that these cracks are forming due to PTL compression that is stronger under land areas. It is also noted that fragmentation is more obvious at low catalyst loadings. Carbon nanofibers (CNFs) introduced to the low loading CL led to better electrical connections in the land

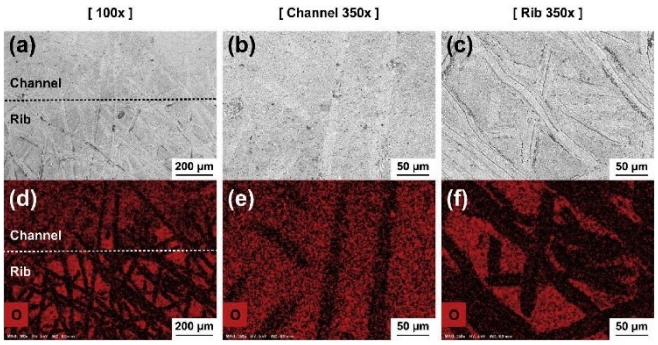

Figure 13. SEM-EDS analysis of a CCM post testing, showing degradation of both land and channel areas. Reproduced with permission from Ref. [129].

no contact region, but further investigation into how to adjust morphology of these structures is needed to further optimize this connection. It should be noted that adjacent PTLs were not characterized after reduction, and so some uncertainty surrounding any redeposition of CCM material exists. Future studies would benefit from evaluation of the PTL in addition to the CCM both before and after testing. Stahler et al. reports compression of the PTL into the MEA also affects hydrogen permeation.[131] The combination of these findings compels further investigation and optimization of the MEA for the PTL-CCM approach to PEMWE manufacturing.

In 2023, Liu et al. investigated the degradation of the MEAs prepared with uncoated and Ir-coated Ti PTLs.[132] This study showed that coating the PTL with Ir protective coating decreases the degree of degradation within the MEA, although degradation is still evident in both cases. This pairs nicely with an earlier study by Kang et al.'s which showed Ir coatings can mitigate local hot spots due to poor thermal conductivity and interfacial contact.[133] In addition to polarization curves and long-term stability tests, Liu et al.'s study utilized STEM-EDS imaging to analyze cross-sections of the MEAs (Figure 14). XPS was used to characterize the catalyst layer to identify changes in the composition of the catalyst. Additionally, F:Ir ratios were

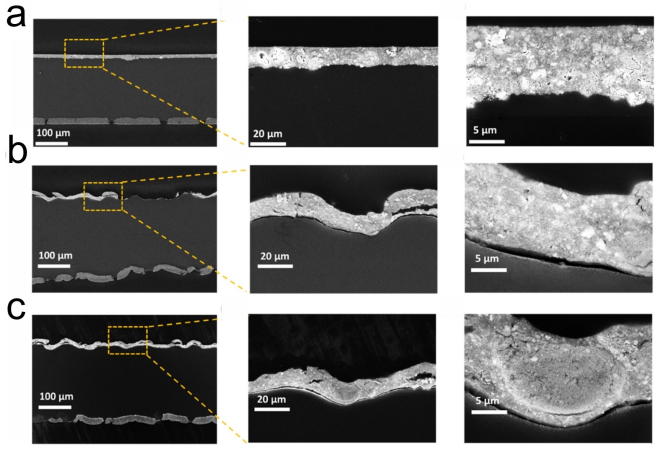

Figure 14. STEM analysis of an MEA a) pristine CCM b) tested with uncoated PTL, and c) tested with Pt coated PTL. Reproduced with permission from Ref. [131].

also calculated to track changes in the relative amount of catalyst and ionomer. The decrease in F:Ir occurs in both the coated and uncoated tested samples, and is likely due to ionomer rearrangement during testing. This result is consistent with previous results reported by Zaccarine et al., which demonstrated that relative amounts of ionomer to catalyst at the surface of the CCM changes after testing, which is expected to affect the CL-PTL interface.[134] AFM was used to compare the relative conductivity and roughness of the two MEAs; results indicated less ionomer rearrangement and degradation on the coated PTL sample. This data implies that significant changes are occurring at the CL/PTL interface due to changes in the catalyst chemistry and distribution of ionomer, its amount and possibly arrangement, and that having a coated PTL has an effect on the severity of these changes.

4.3. Investigation of PTL/CL Interface in PTEs

Several factors motivated the development of PTEs as CCM replacements. These include poor contact between the PTL and the CL, decreased contact due to degradation, and manufacturing costs. XCT has been used to investigate catalyst distribution within the PTE. An extensive review on XCT for electrocatalyst materials was recently published by Lang et al.[135] XCT can provide an important information about catalyst distribution, however, the spatial limitations of XCT become problematic for a detailed and quantitative understanding of catalyst distribution, specifically when investigating the triple phase contact area which is important to the interfacial contact resistance of the PTE. Bierling et al. acknowledge this in a recent study, utilizing cross-sectional imaging in addition to topography to investigate the triple-phase contact area.[136] Reports utilizing XCT on PTEs have reported results for uncoated PTL baselines, likely due to the difficulty of differentiating Ir and Pt with this technique.

The transition from the CCM to the PTE has led to an investigation into the replacement of a protective coating with a multifunctional catalyst/protective coating. Liu et al. reported a PTE where Ir was used multifunctionally, as both a protective coating and a CL.[137] A felt PTL was spray-coated with a protective/catalytic Ir coating, and a half CCM (Nafion and cathode CL) was then pressed into the PTL. It was expected that the ionomer from the Nafion would penetrate the porous Ir layer on the PTL, forming an active area to allow proper catalytic activity. Electrochemical results show that this approach indeed results in catalytic activity, though EIS and calculated resistances indicated that the lack of ionomer within the catalyst layer significantly slows diffusion. Comparison of the Ir PTE to a typical Ir CCM with SEM demonstrated that PTE had a denser Ir structure compared to a more porous morphology of the CCM. Future integration of the catalyst and the PTL in PTE must therefore include integration with the proton conductor; it is not sufficient to simply attach an Ir coated PTL to a Nafion membrane. In a more recent study by Yasutake et al., intermediate catalyst layers and a Ir catalyst integrated PTEs were investigated.[138] Results demonstrate lower activation overvoltage and higher limiting current density, indicating that deposited Ir on PTLs acts as both a catalyst and a conductive coating, eliminating the need for Pt coating. Characterization in this study includes PSV, overvoltage, electrochemical surface area (ECSA), STEM, and SEM analysis.

In a publication by Doan et al. the catalyst coated PTEs were prepared by depositing a variety of loadings of IrO_2/ TiO_2 catalyst ink directly onto a sintered PTL.[139] These catalyst coated PTEs were then combined with an active MEA with a secondary commercially produced iridium oxide catalyst layer. Polarization curves showed that for lower IrO_2/TiO_2 catalyst ink loadings (0.21, 0.39 mg_{Ir}/cm^2), coatings did not improve performance, and in the lowest loaded sample performance even decreased compared to reference samples with uncoated PTL. With higher loadings, performance increased in comparison to the pristine PTL. A follow up study to this further investigates the catalyst precursor ratios.[140] In each study, both XRD and SEM-EDS were used for physical and chemical characterization, confirming the presence of the catalyst materials, IrO_2 and TiO_2. SEM imaging revealed that the catalyst had cracks, exposing the uncoated Ti material. This was more pronounced with the lower loaded coatings and is likely a reason for lower performance. Although these studies provided a comparison between untested and tested series of samples, no comparison to the state-of-the-art coated PTL was shown. The lack of reference reduces the overall information of the novel coating, making comparisons to other PTE fabrication methods more difficult.

Lim et al. adjusted this approach by electrodepositing Pt agglomerates onto a felt PTL, followed by the electrodeposition of Ir.[141] The sequential electrodeposition of Pt and Ir forms a triple layer interface, as confirmed by STEM-EDS (Figure 15). This approach was shown to increase catalytic surface area and demonstrated an increase in the performance; however, the testing parameters of this study were different due to focus on

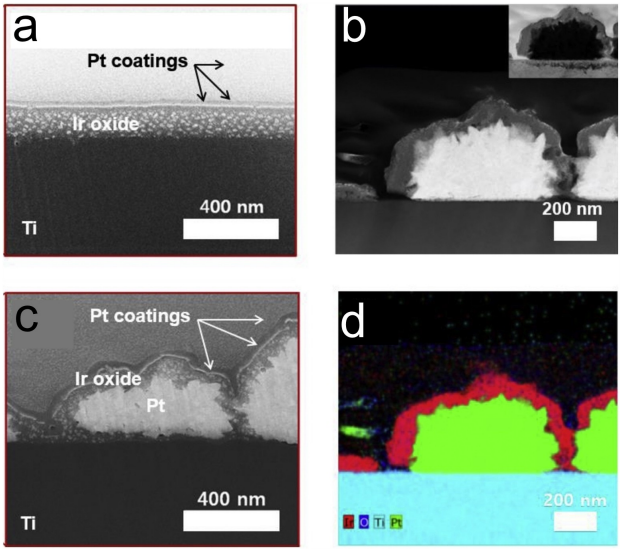

Figure 15. STEM EDS of Pt/Ir coating on PTL Reproduced with permission from Ref. [140].

the development of regenerative fuel cells (URFC). Additionally, the reliance on the CCM type MEA in addition to the catalyst coated PTL will still be too costly for commercial applications.

A recent study by Lee et al. proposes an ionomer-free PTE, which would eliminate two traditional steps of the PTE fabrication process: catalyst synthesis and catalyst-ink fabrication.[142] This approach utilizes physical vapor deposition (PVD), forming a nanosized catalyst layer adhered to the PTL surface. PVD is a scalable and mature industrial process, which could reduce manufacturing time and costs. Additionally, as a line-of-sight technique, PVD offers precise coating only at the interface of the PTL, which could improve catalyst utilization in comparison to techniques such as direct ink coating or electrodeposition. Promisingly, this approach exhibits improved electrode kinetics, and electrode performance improvement stops at 0.0085 mg_{Ir}/cm^2, indicating a smooth application of the catalyst onto the PTL. This statement is aided by SEM and FIB-SEM morphological characterization as well as XCT to visualize catalyst distribution. Extensive chemical characterization of the ionomer-free PTE was reported, including XPS, XRD, and XRF. The combination of these techniques with detailed electrochemical testing provides a comprehensive argument of the ionomer-free PTE approach and highlights the value of providing morphological evaluation along with both surface ad bulk chemical information while reporting new fabrication methods in the literature.

A different approach to the PTE is to utilize novel catalyst components. In 2022, Fan et al. replaced the commonly used Pt electroplated coating with a novel IrO_2-RuO_2-TaO_x coating which acted as both a protective coating and OER catalyst.[143] This novel catalyst coating was deposited directly onto the felt PTL via thermal decomposition. Although a CCM based MEA was still used in addition to this catalyst coated PTL, the anode Ir black loading was reduced, from 2.0 mg cm^2 to 1.0 mg cm^2. Although the novel-coated PTL with had a decreased CCM catalyst loading, it still increased performance (I–V curve), in comparison to the coated PTL with higher CCM Ir catalyst loading, indicating good OER catalytic activity and good conductivity to the MEA. Kang et al. reported a follow up study that investigated iridium nickel oxide directly coated onto the PTL via co-electrodeposition.[144] In this study, five catalyst materials with varied iridium to nickel ratios were tested and compared against Ir and Ir oxide catalysts. Like the previous study, the $Ir_{0.5}Ni_{0.5}O_x$ outperformed the sample made with state-of-the-art catalyst and PTL. Extensive characterization via SEM, FIB-SEM, EDS, XPS, and XRD was conducted, which should be the expectation when reporting development of novel catalyst. Kang et al. also included ICP-MS characterization to confirm Ni : Ir ratios. The use of the same characterization techniques allowed for a good comparison between the two materials. Physicochemical characterization alongside electrochemical results confirmed the feasibility of both materials, although in depth degradation testing and realistic scale-up approaches will be needed for these to be considered for further consideration in commercial applications.

In general, the complexity of variables becomes significantly more difficult to deconvolute when investigating PTEs compared to CCMs. These complexities, along with the exponential rate of PTE publications, prompted the utilization of machine learning to analyze MEA parameters.[145] Although not discussed in detail within the scope of this review, it is important to note that machine learning will be a valuable addition to physiochemical and electrochemical characterization to best identify paths forward with PTEs development.

5. Summary and Outlook

The existing body of research related to PTL characterization has predominantly focused on the morphology of the PTL material, and adjacently, the understanding of the PTL porosity, oxygen pathways, and the two-phase flow mechanism of the system. The paired mechanical engineering and electrochemical performance investigations of the PTL have led to significant findings. These studies highlighted the importance of the interface between the PTL and the CL and motivated investigations of the gradient-like PTL structures. While efforts to optimize the PTL structure are ongoing, the literature suggests that a deeper understanding of the PTL-CL interface is essential for achieving further improvements in PTL performance. The continuing work aims to enhance PTL-CL contact, reduce system degradation, and mitigate two-phase flow blockages.

The electrolysis community is actively researching protective coatings for PTLs to meet the demand for more affordable materials and heightened system efficiency. Exploration into novel materials, lower loadings for catalyst and protective coatings, and the fabrication techniques used for these layers are still under investigation. Reflecting on the preceding discussion, it becomes evident that the addition of the protective layer further complicates the variables that must be explored to evaluate the integration of PTLs with adjacent CLs which is also still evolving.

With so many variables at play, it becomes imperative to further delve beyond the material structure and basic performance testing of the PTL-CL systems to address gaps in understanding the underlying chemistries of these layers, specifically within the integrated system. A better understanding of both protective coatings, catalyst-coated materials, and their integrations is essential for making informed decisions and achieving optimal, sustainable electrolysis systems. Consequently, existing characterization methods in literature need to be combined with other methods that are more commonly used for catalyst studies. The complex structure of coated PTL-CL also demands the development of new techniques to address challenges in the characterization of complex buried interfaces and to qualitatively and quantitatively evaluate variations of the system based on changes in properties of materials, processing, and fabrication conditions.

Continuous improvements in both materials and structures used in PTL-CL systems necessitate corresponding adaptations in the characterization techniques used to study them. The shift in utilization of methods that provide chemical information as opposed to just morphological studies is already happening, as highlighted by expansion of elemental and chemical character-

ization reports discussed in sections 3 and 4 of this review. Though elemental and chemical characterization are more often reported in recent literature, there are variations from study to study that can lead to uncertainty when comparing differences in designs, materials, or application techniques. Notably, there are inconsistencies in the choice of characterization techniques used to assess materials, including SEM vs TEM, three electrode vs stack testing, and whether any additional techniques beyond microscopy and electrochemical testing are employed. The optimization of fabrication techniques and coating materials remains ongoing, with a growing body of research. As more and more research is conducted, it becomes increasingly difficult to compare different materials and fabrication methods. This necessitates the development and adoption of standardized characterization techniques and studies. Due to the wide availability, SEM-EDS can serve as a good standard technique for both visualization and quantitative assessments, but futher investigation into how to properly compare PTEs even with this simple technique must be reported.

In addition to the standardization of current methods, the exploration of diverse characterization techniques commonly used in other scientific fields could enhance future efforts in PTL and PTE development. Despite initial challenges, expanding characterization methods beyond current instrument limitations has proven to lead to major advancements in fundamental and applied research. This was shown by the initial PTL characterization studies where techniques like XCT more often used by other fields were modified and adapted to understand mass transport within the PTLs. For example, XPS could be further utilized for PTE chemical characterization via the use of hard X-rays, especially with the recent development of lab-based hard x-ray instruments. Furthermore, limitations of current bulk and surface characterization techniques towards the understanding of complex buried interfaces are impeding further developments. Although TEM-EDS has been used for this type of characterization, chemical information is limited and a using additional techniques such as ToF SIMS should be further developed. Expanding the capabilities of elemental and chemical characterization techniques is essential to advance our understanding of these critical components in electrolysis systems. Characterization advancements for PEMWEs will inevitably benefit other electrolysis technologies, including alkaline membrane and liquid alkaline systems.

Acknowledgements

This work was authored in part by the National Renewable Energy Laboratory, operated by Alliance for Sustainable Energy, LLC, for the U.S. Department of Energy (DOE) under Contract No. DE-AC36-08GO28308. Funding provided as part of the H2NEW consortium funded by the U.S. Department of Energy Office of Energy Efficiency and Renewable Energy Hydrogen and Fuel Cell Technologies Office. This material is also based upon work supported by the U.S. DOE's Office of Energy Efficiency and Renewable Energy (EERE) under the Hydrogen and Fuel Cell Technologies Office's FY2020 H2@ScaleNewMarkets FOA, Award Number DE-EE0009236. The views expressed in the article do not necessarily represent the views of the DOE or the U.S. Government. The U.S. Government retains and the publisher, by accepting the article for publication, acknowledges that the U.S. Government retains a nonexclusive, paid-up, irrevocable, worldwide license to publish or reproduce the published form of this work, or allow others to do so, for U.S. Government purposes. The Authors acknowledge the H2NEW consortium for useful discussions and acknowledge Dr. Meital Shviro for the useful insights and feedback.

Conflict of Interests

The authors declare no conflict of interest.

Data Availability Statement

Data sharing is not applicable to this article as no new data were created or analyzed in this study.

Keywords: PEMWE · Porous transport layer · Porous transport electrode · Muti-technique characterization · Multi-scale analysis

[1] R. Omrani, B. Shabani, *Int. J. Hydrogen Energy* **2019**, *44*, 3834–3860.
[2] Department of Energy, Technical Report: *International Energy Outlook 2019*, **2019**https://www.eia.gov/outlooks/ieo/.
[3] A. Buttler, H. Spliethoff, *Renew. Sustain. Energy Rev.* **2018**, *82*, 2440–2454.
[4] M. Carmo, D. L. Fritz, J. Mergel, D. Stolten, *Int. J. Hydrogen. Energy* **2013**, *38*, 4901–4934.
[5] A. Mayyas, M. Ruth, B. Pivovar, G. Bender, K. Wipke, *Manufacturing Cost Analysis for Proton Exchange Membrane Water Electrolyzers*, **2019**, www.nrel.gov/publications, https://www.nrel.gov/docs/fy19osti/72740.pdf.
[6] J. R. Rostrup-Nielsen, J. Sehested, J. K. Nørskov, *Advances In Catalysis* **2002**, 65–139.
[7] J. O. Abe, A. P. I. Popoola, E. Ajenifuja, O. M. Popoola, *Int. J. Hydrogen Energy* **2019**, *44*, 15072–15086.
[8] X. Z. Yuan, N. Shaigan, C. Song, M. Aujla, V. Neburchilov, J. T. H. Kwan, D. P. Wilkinson, A. Bazylak, K. Fatih, *Sustain. Energy Fuels* **2022**, *6*, 1824–1853.
[9] P. Shirvanian, F. van Berkel, *Electrochem. Commun.* **2020**, *114*, 106704.
[10] X. Z. Yuan, N. Shaigan, C. Song, M. Aujla, V. Neburchilov, J. T. H. Kwan, D. P. Wilkinson, A. Bazylak, K. Fatih, *Sustain. Energy Fuels* **2022**, *6*, 1824–1853.
[11] H. Yu, N. Danilovic, Y. Wang, W. Willis, A. Poozhikunnath, L. Bonville, C. Capuano, K. Ayers, R. Maric, *Appl. Catal. B* **2018**, *239*, 133–146.
[12] S. Shiva Kumar, V. Himabindu, *Mater. Sci. Energy Technol.* **2019**, *2*, 442–454.
[13] S. Marini, P. Salvi, P. Nelli, R. Pesenti, M. Villa, M. Berrettoni, G. Zangari, Y. Kiros, *Electrochim. Acta* **2012**, *82*, 384–391.
[14] Y. Chen, C. Liu, J. Xu, C. Xia, P. Wang, B. Y. Xia, Y. Yan, X. Wang, *Small Struct.* **2022**, *4*, 2200130.
[15] S. Toghyani, S. Fakhradini, E. Afshari, E. Baniasadi, M. Y. Abdollahzadeh Jamalabadi, M. Safdari Shadloo, *Int. J. Hydrogen Energy* **2019**, *44*, 6403–6414.
[16] X. Z. Yuan, N. Shaigan, C. Song, M. Aujla, V. Neburchilov, J. T. H. Kwan, D. P. Wilkinson, A. Bazylak, K. Fatih, *Sustain. Energy Fuels* **2022**, *6*, 1824–1853.
[17] O. Schmidt, A. Gambhir, I. Staffell, A. Hawkes, J. Nelson, S. Few, *Int. J. Hydrogen Energy* **2017**, *42*, 30470–30492.
[18] M. Carmo, D. L. Fritz, J. Mergel, D. Stolten, *Int. J. Hydrogen Energy* **2013**, *38*, 4901–4934.

[19] U. Babic, M. Suermann, F. N. Büchi, L. Gubler, T. J. Schmidt, *J. Electrochem. Soc.* **2017**, *164*, F387–F399.
[20] M. N. I. Salehmin, T. Husaini, J. Goh, A. B. Sulong, *Energy Convers. Manag.* **2022**, *268*, 115985.
[21] P. Millet, N. Mbemba, S. A. Grigoriev, V. N. Fateev, A. Aukauloo, C. Etiévant, *Int. J. Hydrogen Energy* **2011**, *36*, 4134–4142.
[22] Ö. F. Selamet, F. Becerikli, M. D. Mat, Y. Kaplan, *Int. J. Hydrogen Energy* **2011**, *36*, 11480–11487.
[23] Dmitri Bessarabov, Haijiang Wang, Hui Li, Nana Zhao, *PEM Electrolysis for Hydrogen Production: Principles and Applications*, CRC Press, United Kingdom **2016**.
[24] P. Holzapfel, M. Bühler, C. Van Pham, F. Hegge, T. Böhm, D. McLaughlin, M. Breitwieser, S. Thiele, *Electrochem. Commun.* **2020**, *110*, 106640.
[25] S. Cherevko, A. R. Zeradjanin, A. A. Topalov, N. Kulyk, I. Katsounaros, K. J. J. Mayrhofer, *ChemCatChem* **2014**, *6*, 2219–2223.
[26] C. Van Pham, D. Escalera-López, K. Mayrhofer, S. Cherevko, S. Thiele, *Adv. Energy Mater.* **2021**, *11*, 2101998.
[27] H. Yoon, B. Ju, D. Kim, *Battery Energy* **2023**, *2*, 20230017.
[28] Z. Chen, L. Guo, L. Pan, T. Yan, Z. He, Y. Li, C. Shi, Z. F. Huang, X. Zhang, J. J. Zou, *Adv. Energy Mater.* **2022**, *12*, 2103670.
[29] B. Tamilarasi, K. P. Jithul, J. Pandey, *Int. J. Hydrogen Energy* **2024**, *58*, 556–582.
[30] T. L. Doan, H. E. Lee, S. S. H. Shah, M. J. Kim, C. H. Kim, H. S. Cho, T. Kim, *Int. J. Energy Res.* **2021**, *45*, 14207–14220.
[31] M. Suermann, K. Takanohashi, A. Lamibrac, T. J. Schmidt, F. N. Büchi, *J. Electrochem. Soc.* **2017**, *164*, F973–F980.
[32] M. Pourbaix, *Atlas of Electrochemical Equilibria In-Aqueous Solutions*, National Association of Corrosion Engineers, Huston, TX **1974**.
[33] D. Bessarabov, P. Millet, *PEM Water Electrolysis*, Elsevier, Amsterdam **2018**, 61–94.
[34] M. Prestat, *J. Power Sources* **2023**, *556*, 232469.
[35] Z. Kang, T. Schuler, Y. Chen, M. Wang, F. Y. Zhang, G. Bender, *Electrochim. Acta* **2022**, *429*, 140942.
[36] P. Trinke, B. Bensmann, R. Hanke-Rauschenbach, *Electrochem. Commun.* **2017**, *82*, 98–102.
[37] C. Rozain, E. Mayousse, N. Guillet, P. Millet, *Appl. Catal .B* **2016**, *182*, 153–160.
[38] M. Bernt, H. A. Gasteiger, *J. Electrochem. Soc.* **2016**, *163*, F3179–F3189.
[39] S. A. Mauger, M. Wang, F. C. Cetinbas, M. J. Dzara, J. Park, D. J. Myers, R. K. Ahluwalia, S. Pylypenko, L. Hu, S. Litster, K. C. Neyerlin, M. Ulsh, *J. Power Sources* **2021**, *506*, 230039.
[40] S. A. Mauger, J. R. Pfeilsticker, M. Wang, S. Medina, A. C. Yang-Neyerlin, K. C. Neyerlin, C. Stetson, S. Pylypenko, M. Ulsh, *J. Power Sources* **2020**, *450*, 227581.
[41] B. S. Lee, S. H. Ahn, H. Y. Park, I. Choi, S. J. Yoo, H. J. Kim, D. Henkensmeier, J. Y. Kim, S. Park, S. W. Nam, K. Y. Lee, J. H. Jang, *Appl. Catal. B* **2015**, *179*, 285–291.
[42] S. Choe, B. S. Lee, M. K. Cho, H. J. Kim, D. Henkensmeier, S. J. Yoo, J. Y. Kim, S. Y. Lee, H. S. Park, J. H. Jang, *Appl. Catal. B* **2018**, *226*, 289–294.
[43] F. M. Sapountzi, S. C. Divane, E. I. Papaioannou, S. Souentie, C. G. Vayenas, *J. Electroanal. Chem.* **2011**, *662*, 116–122.
[44] S. A. Grigoriev, P. Millet, S. A. Volobuev, V. N. Fateev, *Int. J. Hydrogen Energy* **2009**, *34*, 4968–4973.
[45] M. Bühler, P. Holzapfel, D. McLaughlin, S. Thiele, *J. Electrochem Soc.* **2019**, *166*, F1070–F1078.
[46] M. Bühler, F. Hegge, P. Holzapfel, M. Bierling, M. Suermann, S. Vierrath, S. Thiele, *J Mater. Chem. A Mater.* **2019**, *7*, 26984–26995.
[47] Department of Energy, *Final Technical Report-RPTXXXX Project Title: High Efficiency PEM Water Electrolysis Enabled by Advanced Catalysts, Membranes and Processes*, **2021**, https://doi.org/10.2172/1963948.
[48] C. Qiu, Z. Xu, F. Y. Chen, H. Wang, *ACS Catal.* **2024**, *14*, 921–954.
[49] C. Wang, K. Lee, C. P. Liu, D. Kulkarni, P. Atanassov, X. Peng, I. V. Zenyuk, *Int. Mater. Rev.* **2024**, *69*, 3–18.
[50] J. H. Russell, L. J. J.Nuttall. A. P. Fickett, *Am. Chem. Soc. Div. Fuel Chem.* **1973**, *18*, 24–40.
[51] P. Trinke, G. P. Keeley, M. Carmo, B. Bensmann, R. Hanke-Rauschenbach, *J. Electrochem. Soc.* **2019**, *166*, F465–F471.
[52] S. Siracusano, V. Baglio, A. Di Blasi, N. Briguglio, A. Stassi, R. Ornelas, E. Trifoni, V. Antonucci, A. S. Aric, *Int. J. Hydrogen Energy* **2010**, *35*, 5558–5568.
[53] E. Borgardt, L. Giesenberg, M. Reska, M. Müller, K. Wippermann, M. Langemann, W. Lehnert, D. Stolten, *Int. J. Hydrogen Energy* **2019**, *44*, 23556–23567.
[54] F. J. Hackemüller, E. Borgardt, O. Panchenko, M. Müller, M. Bram, *Adv. Eng. Mater.* **2019**, *21*, 1801201.
[55] F. Arbabi, A. Kalantarian, R. Abouatallah, R. Wang, J. S. Wallace, A. Bazylak, *J. Power Sources* **2014**, *258*, 142–149.
[56] H. Ito, T. Maeda, A. Nakano, C. M. Hwang, M. Ishida, A. Kato, T. Yoshida, *Int. J. Hydrogen Energy* **2012**, *37*, 7418–7428.
[57] H. Ito, T. Maeda, A. Nakano, A. Kato, T. Yoshida, *Electrochim. Acta* **2013**, *100*, 242–248.
[58] H. Li, T. Fujigaya, H. Nakajima, A. Inada, K. Ito, *J. Power Sources* **2016**, *332*, 16–23.
[59] L. Wan, M. Pang, J. Le, Z. Xu, H. Zhou, Q. Xu, B. Wang, *Nat. Commun.* **2022**, *13*, 7956.
[60] R. J. Ouimet, J. L. Young, T. Schuler, G. Bender, G. M. Roberts, K. E. Ayers, *Front. Energy. Res.* **2022**, *10*, 911077.
[61] K. Bromberger, J. Ghinaiya, T. Lickert, A. Fallisch, T. Smolinka, *Int. J. Hydrogen Energy* **2018**, *43*, 2556–2569.
[62] R. J. Ouimet, J. L. Young, T. Schuler, G. Bender, G. M. Roberts, K. E. Ayers, *Front. Energy Res.* **2022**, *10*, 911077.
[63] F. Arbabi, H. Montazeri, R. Abouatallah, R. Wang, A. Bazylak, *J. Electrochem. Soc.* **2016**, *163*, F3062–F3069.
[64] I. Dedigama, P. Angeli, K. Ayers, J. B. Robinson, P. R. Shearing, D. Tsaoulidis, D. J. L. Brett, *Int. J. Hydrogen Energy* **2014**, *39*, 4468–4482.
[65] I. Dedigama, P. Angeli, N. Van Dijk, J. Millichamp, D. Tsaoulidis, P. R. Shearing, D. J. L. Brett, *J. Power Sources* **2014**, *265*, 97–103.
[66] H. Markötter, I. Manke, R. Kuhn, T. Arlt, N. Kardjilov, M. P. Hentschel, A. Kupsch, A. Lange, C. Hartnig, J. Scholta, J. Banhart, *J. Power Sources* **2012**, *219*, 120–125.
[67] M. A. Hickner, N. P. Siegel, K. S. Chen, D. S. Hussey, D. L. Jacobson, M. Arif, *J. Electrochem. Soc.* **2008**, *155*, B427.
[68] R. S. Fu, U. Pasaogullari, T. Shiomi, Y. Tabuchi, D. S. Hussey, D. L. Jacobson, *J. Electrochem. Soc.* **2012**, *159*, F545–F553.
[69] P. Boillat, G. Frei, E. H. Lehmann, G. G. Scherer, A. Wokaun, *Electrochem. Solid-State Lett.* **2010**, *13*, B25.
[70] K. Mishima, T. Hibiki, K. Mishima, T. Hibiki, *Int. J. Multiphase Flow* **1996**, *22*, 703–712.
[71] O. F. Selamet, U. Pasaogullari, D. Spernjak, D. S. Hussey, D. L. Jacobson, M. D. Mat, *Int. J. Hydrogen Energy* **2013**, *38*, 5823–5835.
[72] J. Seweryn, J. Biesdorf, T. J. Schmidt, P. Boillat, *J. Electrochem. Soc.* **2016**, *163*, F3009–F3011.
[73] O. Panchenko, E. Borgardt, W. Zwaygardt, F. J. Hackemüller, M. Bram, N. Kardjilov, T. Arlt, I. Manke, M. Müller, D. Stolten, W. Lehnert, *J. Power Sources* **2018**, *390*, 108–115.
[74] C. H. Lee, J. K. Lee, B. Zhao, K. F. Fahy, J. M. LaManna, E. Baltic, D. S. Hussey, D. L. Jacobson, V. P. Schulz, A. Bazylak, *J. Power Sources* **2020**, *446*, 227312.
[75] R. Lenormand, E. Touboul, C. Zarcone, *J. Fluid Mech.* **1988**, *189*, 165–187.
[76] C. Minnaar, F. De Beer, D. Bessarabov, *Energy Fuels* **2020**, *34*, 1014–1023.
[77] M. Maier, J. Dodwell, R. Ziesche, C. Tan, T. Heenan, J. Majasan, N. Kardjilov, H. Markötter, I. Manke, L. Castanheira, G. Hinds, P. R. Shearing, D. J. L. Brett, *J Power Sources* **2020**, *455*, 227968.
[78] M. Zlobinski, T. Schuler, F. N. Büchi, T. J. Schmidt, P. Boillat, *J. Electrochem. Soc.* **2020**, *167*, 084509.
[79] B. Zhao, C. H. Lee, J. K. Lee, K. F. Fahy, J. M. LaManna, E. Baltic, D. L. Jacobson, D. S. Hussey, A. Bazylak, *Cell. Rep. Phys. Sci.* **2021**, *2*, 100580.
[80] I. Manke, C. Hartnig, M. Grünerbel, W. Lehnert, N. Kardjilov, A. Haibel, A. Hilger, J. Banhart, H. Riesemeier, *Appl. Phys. Lett.* **2007**, *90*, 174105.
[81] T. Sasabe, P. Deevanhxay, S. Tsushima, S. Hirai, *J. Power Sources* **2011**, *196*, 8197–8206.
[82] P. Deevanhxay, T. Sasabe, S. Tsushima, S. Hirai, *J. Power Sources* **2013**, *230*, 38–43.
[83] J. Haußmann, H. Markötter, R. Alink, A. Bauder, K. Dittmann, I. Manke, J. Scholta, *J. Power Sources* **2013**, *239*, 611–622.
[84] M. A. Hoeh, T. Arlt, I. Manke, J. Banhart, D. L. Fritz, W. Maier, W. Lehnert, *Electrochem. Commun.* **2015**, *55*, 55–59.
[85] E. Leonard, A. D. Shum, S. Normile, D. C. Sabarirajan, D. G. Yared, X. Xiao, I. V. Zenyuk, *Electrochim. Acta* **2018**, *276*, 424–433.
[86] E. Leonard, A. D. Shum, N. Danilovic, C. Capuano, K. E. Ayers, L. M. Pant, A. Z. Weber, X. Xiao, D. Y. Parkinson, I. V. Zenyuk, *Sustain. Energy Fuels* **2020**, *4*, 921–931.
[87] L. Vásárhelyi, Z. Kónya, Kukovecz, R. Vajtai, *Mater. Today Adv.* **2020**, *8*, 100084.
[88] L. Zielke, A. Fallisch, N. Paust, R. Zengerle, S. Thiele, *RSC Adv.* **2014**, *4*, 58888–58894.

[89] J. O. Majasan, F. Iacoviello, P. R. Shearing, D. J. L. Brett, in *Energy Procedia*, Elsevier Ltd, Amsterdam **2018**, 111–119.
[90] J. O. Majasan, F. Iacoviello, J. I. S. Cho, M. Maier, X. Lu, T. P. Neville, I. Dedigama, P. R. Shearing, D. J. L. Brett, *Int. J. Hydrogen Energy* **2019**, *44*, 19519–19532.
[91] T. Schuler, R. De Bruycker, T. J. Schmidt, F. N. Büchi, *J. Electrochem. Soc.* **2019**, *166*, F270–F281.
[92] T. Schuler, T. J. Schmidt, F. N. Büchi, *J. Electrochem. Soc.* **2019**, *166*, F555–F565.
[93] A. S. Pushkarev, I. V. Pushkareva, M. A. Solovyev, M. Prokop, T. Bystron, S. K. Rajagopalan, K. Bouzek, S. A. Grigoriev, *Electrochim. Acta* **2021**, *399*, 139436.
[94] X. Peng, P. Satjaritanun, Z. Taie, L. Wiles, A. Keane, C. Capuano, I. V. Zenyuk, N. Danilovic, *Adv. Sci.* **2021**, *8*, 2102950.
[95] C. C. Weber, T. Schuler, R. De Bruycker, L. Gubler, F. N. Büchi, S. De Angelis, *J. Power Sources Adv.* **2022**, *15*, 100095.
[96] Q. Chen, Y. Wang, F. Yang, H. Xu, *Int. J. Hydrogen Energy* **2020**, *45*, 32984–32994.
[97] P. Satjaritanun, M. O'Brien, D. Kulkarni, S. Shimpalee, C. Capuano, K. E. Ayers, N. Danilovic, D. Y. Parkinson, I. V. Zenyuk, *iScience* **2020**, *23*, 101783.
[98] S. De Angelis, T. Schuler, M. A. Charalambous, F. Marone, T. J. Schmidt, F. N. Büchi, *J. Mater. Chem. A Mater.* **2021**, *9*, 22102–22113.
[99] A. Kellenberger, N. Vaszilcsin, D. Duca, M. L. Dan, N. Duteanu, S. Stiber, T. Morawietz, I. Biswas, S. A. Ansar, P. Gazdzicki, F. J. Wirkert, J. Roth, U. Rost, M. Brodmann, A. S. Gago, K. A. Friedrich, *Materials* **2022**, *15*, 1628.
[100] M. Langemann, D. L. Fritz, M. Müller, D. Stolten, *Int J Hydrogen Energy* **2015**, 11385–11391.
[101] L. Wang, J. Sun, J. Sun, Y. Lv, S. Li, S. Ji, Z. Wen, *J. Power Sources* **2012**, *199*, 195–200.
[102] H. Wakayama, K. Yamazaki, *ACS Omega* **2021**, *6*, 4161–4166.
[103] H. Y. Jung, S. Y. Huang, B. N. Popov, *J. Power Sources* **2010**, *195*, 1950–1956.
[104] C. Rakousky, U. Reimer, K. Wippermann, M. Carmo, W. Lueke, D. Stolten, *J. Power Sources* **2016**, *326*, 120–128.
[105] C. Rakousky, G. P. Keeley, K. Wippermann, M. Carmo, D. Stolten, *Electrochim. Acta* **2018**, *278*, 324–331.
[106] Z. Kang, J. Mo, G. Yang, Y. Li, D. A. Talley, S. T. Retterer, D. A. Cullen, T. J. Toops, M. P. Brady, G. Bender, B. S. Pivovar, J. B. Green, F. Y. Zhang, *Appl. Energy* **2017**, *206*, 983–990.
[107] N. F. Daudt, A. D. Schneider, E. R. Arnemann, C. J. Scheuer, L. S. Dorneles, L. F. Schelp, *J. Mater. Eng. Perform.* **2020**, *29*, 5174–5183.
[108] L. Wang, J. Sun, J. Sun, Y. Lv, S. Li, S. Ji, Z. Wen, *J. Power Sources* **2012**, *199*, 195–200.
[109] M. Li, S. Luo, C. Zeng, J. Shen, H. Lin, C. Cao, *Corros. Sci.* **2004**, *46*, 1369–1380.
[110] J. Mo, S. M. Steen, F. Y. Zhang, T. J. Toops, M. P. Brady, J. B. Green, *Int. J. Hydrogen Energy* **2015**, *40*, 12506–12511.
[111] J. Mo, S. Steen, Z. Kang, G. Yang, D. A. Taylor, Y. Li, T. J. Toops, M. P. Brady, S. T. Retterer, D. A. Cullen, J. B. Green, F. Y. Zhang, *Int. J. Hydrogen Energy* **2017**, *42*, 27343–27349.
[112] J. L. Young, Z. Kang, F. Ganci, S. Madachy, G. Bender, *Electrochem. Commun.* **2021**, *124*, 106941.
[113] S. Stiber, N. Sata, T. Morawietz, S. A. Ansar, T. Jahnke, J. K. Lee, A. Bazylak, A. Fallisch, A. S. Gago, K. A. Friedrich, *Energy Environ. Sci.* **2022**, *15*, 109–122.
[114] H. Becker, L. Castanheira, G. Hinds, *J. Power Sources* **2020**, *448*, 227563.
[115] H. Becker, E. J. F. Dickinson, X. Lu, U. Bexell, S. Proch, C. Moffatt, M. Stenström, G. Smith, G. Hinds, *Energy Environ. Sci.* **2022**, *15*, 2508–2518.
[116] T. Bystron, M. Vesely, M. Paidar, G. Papakonstantinou, K. Sundmacher, B. Bensmann, R. Hanke-Rauschenbach, K. Bouzek, *J. Appl. Electrochem.* **2018**, *48*, 713–723.
[117] B. C. Lamartine, T. W. Haas, J. S. Solomon, *Appl. Surf. Sci. (1977–1985)*, **1980**, *4*, 537–555.
[118] T. Bautkinova, N. Utsch, T. Bystron, M. Lhotka, M. Kohoutkova, M. Shviro, K. Bouzek, *J. Power Sources* **2023**, *565*, 232913.
[119] C. Liu, M. Carmo, G. Bender, A. Everwand, T. Lickert, J. L. Young, T. Smolinka, D. Stolten, W. Lehnert, *Electrochem. Commun.* **2018**, *97*, 96–99.
[120] C. Liu, M. Shviro, A. S. Gago, S. F. Zaccarine, G. Bender, P. Gazdzicki, T. Morawietz, I. Biswas, M. Rasinski, A. Everwand, R. Schierholz, J. Pfeilsticker, M. Müller, P. P. Lopes, R. A. Eichel, B. Pivovar, S. Pylypenko, K. A. Friedrich, W. Lehnert, M. Carmo, *Adv. Energy Mater.* **2021**, *11*, 2002926.
[121] J. K. Lee, C. H. Lee, K. F. Fahy, P. J. Kim, J. M. LaManna, E. Baltic, D. L. Jacobson, D. S. Hussey, S. Stiber, A. S. Gago, K. A. Friedrich, A. Bazylak, *Energy Convers. Manag.* **2020**, *226*, 113545.
[122] T. Schuler, J. M. Ciccone, B. Krentscher, F. Marone, C. Peter, T. J. Schmidt, F. N. Büchi, *Adv. Energy Mater.* **2020**, *10*, 1903216.
[123] M. Zlobinski, T. Schuler, F. N. Büchi, T. J. Schmidt, P. Boillat, *J. Electrochem. Soc.* **2021**, *168*, 014505.
[124] Z. Kang, G. Yang, J. Mo, S. Yu, D. A. Cullen, S. T. Retterer, T. J. Toops, M. P. Brady, G. Bender, B. S. Pivovar, J. B. Green, F. Y. Zhang, *Int. J. Hydrogen Energy* **2018**, *43*, 14618–14628.
[125] Z. Kang, S. Yu, G. Yang, Y. Li, G. Bender, B. S. Pivovar, J. B. Green, F. Y. Zhang, *Electrochim. Acta* **2019**, *316*, 43–51.
[126] S. Stiber, H. Balzer, A. Wierhake, F. J. Wirkert, J. Roth, U. Rost, M. Brodmann, J. K. Lee, A. Bazylak, W. Waiblinger, A. S. Gago, K. A. Friedrich, *Adv. Energy Mater.* **2021**, *11*, 2100630.
[127] P. J. Kim, J. K. Lee, C. H. Lee, K. F. Fahy, P. Shrestha, K. Krause, H. W. Shafaque, A. Bazylak, *Electrochim. Acta* **2021**, *373*, 137879.
[128] H. Nakajima, H. Ekström, A. Shima, Y. Sone, G. Lindbergh, *ECS Trans.* **2023**, *112*, 273–281.
[129] J. Lopata, Z. Kang, J. Young, G. Bender, J. W. Weidner, S. Shimpalee, *J. Electrochem. Soc.* **2020**, *167*, 064507.
[130] J. Kwen, G. Doo, S. Choi, H. Guim, S. Yuk, D. H. Lee, D. W. Lee, J. Hyun, H. T. Kim, *Int. J. Hydrogen Energy* **2022**, *47*, 14017–14026.
[131] M. Stähler, A. Stähler, F. Scheepers, M. Carmo, W. Lehnert, D. Stolten, *Int. J. Hydrogen Energy* **2020**, *45*, 4008–4014.
[132] C. Liu, M. Shviro, G. Bender, A. S. Gago, T. Morawietz, M. Dzara, I. Biswas, P. Gazdzicki, Z. Kang, S. Zaccarine, S. Pylypenko, K. A. Friedrich, M. Carmo, W. Lehnert, *J Electrochem. Soc.* **2023**, *170*, 034508.
[133] Z. Kang, S. M. Alia, J. L. Young, G. Bender, *Electrochim. Acta* **2020**, *354*, 136641.
[134] S. F. Zaccarine, M. Shviro, J. N. Weker, M. J. Dzara, J. Foster, M. Carmo, S. Pylypenko, *J Electrochem. Soc.* **2022**, *169*, 064502.
[135] J. T. Lang, D. Kulkarni, C. W. Foster, Y. Huang, M. A. Sepe, S. Shimpalee, D. Y. Parkinson, I. V. Zenyuk, *Chem. Rev.* **2023**, *123*, 9880–9914.
[136] M. Bierling, D. McLaughlin, B. Mayerhöfer, S. Thiele, *Adv. Energy Mater.* **2023**, *13*, 2203636.
[137] C. Liu, K. Wippermann, M. Rasinski, Y. Suo, M. Shviro, M. Carmo, W. Lehnert, *ACS Appl. Mater. Interfaces* **2021**, *13*, 16182–16196.
[138] M. Yasutake, Z. Noda, J. Matsuda, S. M. Lyth, M. Nishihara, K. Ito, A. Hayashi, K. Sasaki, *J. Electrochem. Soc.* **2023**, *170*, 124507.
[139] T. L. Doan, H. E. Lee, M. J. Kim, W. C. Cho, H. S. Cho, T. Kim, *J. Power Sources* **2022**, *533*, 231370.
[140] T. L. Doan, T. N. Nguyen, Y. S. Jung, C. Lee, M. J. Kim, S. Lee, H. S. Cho, T. Kim, *Int. J. Hydrogen Energy* **2024**, *55*, 839–847.
[141] A. Lim, J. Kim, H. J. Lee, H. J. Kim, S. J. Yoo, J. H. Jang, H. Young Park, Y. E. Sung, H. S. Park, *Appl. Catal. B* **2020**, *272*, 118955.
[142] J. K. Lee, G. Anderson, A. W. Tricker, F. Babbe, A. Madan, D. A. Cullen, J. D. Arregui-Mena, N. Danilovic, R. Mukundan, A. Z. Weber, X. Peng, *Nat. Commun.* **2023**, *14*, 4592.
[143] Z. Fan, H. Yu, G. Jiang, D. Yao, S. Sun, J. Chi, B. Qin, Z. Shao, *Int. J. Hydrogen Energy* **2022**, *47*, 18963–18971.
[144] S. Y. Kang, J. E. Park, G. Y. Jang, C. Choi, Y. H. Cho, Y. E. Sung, *Adv. Mater. Interfaces* **2023**, *10*, .
[145] Y. Zhang, A. Tan, Z. Yuan, K. Zhao, X. Shi, P. Liu, J. Liu, *Ind. Eng. Chem. Res.* **2024**, *63*, 1409–1421.

Manuscript received: May 22, 2024
Revised manuscript received: July 19, 2024
Version of record online: September 20, 2024